NASA TECHNICAL NOTE

NASA TN D-7463

NASA TN D-7463

SIMULATION OF DECELERATING LANDING APPROACHES ON AN EXTERNALLY BLOWN FLAP STOL TRANSPORT AIRPLANE

by William D. Grantham, Luat T. Nguyen, and Perry L. Deal

Langley Research Center
Hampton, Va. 23665

NATIONAL AERONAUTICS AND SPACE ADMINISTRATION • WASHINGTON, D. C. • MAY 1974

1. Report No.	2. Government Accession No.	3. Recipient's Catalog No.
NASA TN D-7463		

4. Title and Subtitle	5. Report Date
SIMULATION OF DECELERATING LANDING APPROACHES ON AN EXTERNALLY BLOWN FLAP STOL TRANSPORT AIRPLANE	May 1974
	6. Performing Organization Code

7. Author(s)	8. Performing Organization Report No.
William D. Grantham, Luat T. Nguyen, and Perry L. Deal	L-9242
	10. Work Unit No. 760-61-02-01

9. Performing Organization Name and Address	11. Contract or Grant No.
NASA Langley Research Center Hampton, Va. 23665	
	13. Type of Report and Period Covered Technical Note

12. Sponsoring Agency Name and Address	14. Sponsoring Agency Code
National Aeronautics and Space Administration Washington, D.C. 20546	

15. Supplementary Notes

16. Abstract

A fixed-base simulator program was conducted to define the problems and methods of solution associated with performing decelerating landing approaches on a representative STOL transport having a high wing and equipped with an external-flow jet flap in combination with four high-bypass-ratio fan-jet engines. Real-time digital simulation techniques were used. The computer was programed with equations of motion for six degrees of freedom and the aerodynamic inputs were based on measured wind-tunnel data. The pilot's task was to capture the localizer and the glide slope and to maintain them as closely as possible while decelerating from an initial airspeed of 140 knots to a final airspeed of 75 knots, while under IFR conditions.

17. Key Words (Suggested by Author(s))	18. Distribution Statement
STOL landing approach Decelerating approaches Piloting techniques Aircraft noise Curved-descending approaches	Unclassified – Unlimited STAR Category 02

19. Security Classif. (of this report)	20. Security Classif. (of this page)	21. No. of Pages	22. Price*
Unclassified	Unclassified	48	$3.25

*For sale by the National Technical Information Service, Springfield, Virginia 22151

SIMULATION OF DECELERATING LANDING APPROACHES ON AN EXTERNALLY BLOWN FLAP STOL TRANSPORT AIRPLANE

By William D. Grantham, Luat T. Nguyen, and Perry L. Deal
Langley Research Center

SUMMARY

A fixed-base simulator program was conducted to define the problems and methods of solution associated with performing decelerating landing approaches on a representative STOL transport having a high wing and equipped with an external-flow jet flap in combination with four high-bypass-ratio fan-jet engines. Real-time digital simulation techniques were used. The computer was programed with equations of motion for six degrees of freedom and the aerodynamic inputs were based on measured wind-tunnel data. The pilot's task was to capture the localizer and the glide slope and to maintain them as closely as possible while decelerating from an initial airspeed of 140 knots to a final airspeed of 75 knots, while under IFR conditions.

The results of the study indicated that when flying a 7.5^{o} glide slope, the deceleration to 75 knots should be completed at an altitude of no less than approximately 152 m (500 ft). It was also determined that none of the four deceleration piloting techniques allowed sustained deceleration rates greater than approximately 1.52 m/sec^2 (5 ft/sec^2) due to the limitation of the automatic speed controller; for one of the techniques, the maximum sustained deceleration rate attainable was less than 0.61 m/sec^2 (2 ft/sec^2).

The simulated winds and turbulence had little effect on the pilot's ability to perform the deceleration. Also, curved-descending approaches had no significant effects on the deceleration procedures investigated in this study.

When a decelerating approach was made, the amount of time required to attain an altitude of 152 m (500 ft), starting from an altitude of 1219 m (4000 ft), was found to be as much as 1.5 minutes less than the amount of time required for a constant 75-knot approach speed.

Some of the deceleration procedures investigated in this study should be acceptable from a passenger comfort standpoint for deceleration rates as high as 1.22 m/sec^2 (4 ft/sec^2).

INTRODUCTION

The STOL aircraft will require the capability to operate in congested airspace without interfering with existing CTOL operations. It is apparent, however, that STOL aircraft flying at 70- to 80-knot approach speeds and glide-slope angles of 7.5° or steeper cannot be efficiently integrated into the same approach patterns with jet transports flying at speeds of about 140 knots and glide-slope angles of 3° or less. It therefore appears that future STOL airplanes may have to fly decelerating approaches, if for no other reason than the traffic control problem. The term "decelerating approach" as used in this study, refers to a landing approach that starts at a relatively high speed (140 knots) and altitude (as high as 1219 m (4000 ft)), followed by a constant deceleration to the landing speed (75 knots) at a point "near" the runway. Potential advantages to performing decelerating approaches other than for traffic control include: (1) less time required on the approach; (2) decrease in fuel consumption; and (3) decrease in the ground noise level realized due to the lower power settings.

The present simulation program was conducted to define the problems and methods of solution associated with performing decelerating approaches on a representative STOL transport airplane. The study was conducted with a fixed-base cockpit and a visual display of an airport runway and the surrounding area (shown in ref. 1). Real-time digital simulation techniques were used in the study. The computer was programed with equations of motion for six degrees of freedom and the aerodynamic coefficients were based on measured wind-tunnel data. (See refs. 2 to 4.)

Some of the specific objectives of the investigation were as follows:

1. Determine the maximum acceptable rate of descent below various altitudes.

2. Determine the best techniques for controlling airspeed and glide slope during the deceleration period of the landing approach.

3. Determine effects of various levels of deceleration.

4. Determine effects of atmospheric turbulence and/or various wind conditions on the deceleration techniques.

5. Investigate the effects of deceleration techniques on ground noise level.

SYMBOLS AND DEFINITIONS

In order to facilitate international usage of the data presented, dimensional quantities are presented in both the International System of Units (SI) and U.S. Customary Units. The measurements and calculations were made in U.S. Customary Units. Dots over symbols denote differentiation with respect to time.

b	wing span, m (ft)
C_l	rolling-moment coefficient
C_m	pitching-moment coefficient
C_n	yawing-moment coefficient
C_T	thrust coefficient
C_X	longitudinal-force coefficient
C_Y	side-force coefficient
C_Z	vertical-force coefficient
c	local chord, m (ft)
$\bar{c}$	mean aerodynamic chord, m (ft)
g	acceleration due to gravity, 1g = 9.8 m/sec^2 (32.2 ft/sec^2)
h	altitude, m (ft)
I_X, I_Y, I_Z	moments of inertia about X, Y, and Z body axes, respectively, kg-m^2 (slug-ft^2)
I_{XZ}	product of inertia, kg-m^2 (slug-ft^2)
p,q,r	rolling, pitching, and yawing angular velocities, respectively, deg/sec or rad/sec
T	thrust, N (lbf)
t	time, sec
V	airspeed, knots (1 knot = 0.5144 m/sec)
X,Y,Z	body reference axes

α angle of attack, deg

β angle of sideslip, deg

γ flight-path angle, deg

δ_a aileron deflection, positive for right roll command, deg

δ_{f1} deflection of forward segment of trailing-edge flap, deg

δ_{f2} deflection of middle segment of trailing-edge flap, deg

δ_{f3} deflection of rearward segment of trailing-edge flap, deg

δ_r rudder deflection, positive for left yaw command, deg

δ_s asymmetric deflection of spoilers for roll control, positive for right roll command, deg

δ_{sp} symmetric deflection of spoilers for lift control, deg

δ_t horizontal-tail deflection, positive when trailing edge is deflected down, deg

ϵ_{zh} glide-slope error, m (ft)

θ pitch angle, deg

The aerodynamic derivatives are as follows:

$$C_{l_p} = \frac{\partial C_l}{\partial \frac{pb}{2V}} \qquad C_{l_r} = \frac{\partial C_l}{\partial \frac{rb}{2V}} \qquad C_{l_\beta} = \frac{\partial C_l}{\partial \beta}$$

$$C_{l_{\delta_a}} = \frac{\partial C_l}{\partial \delta_a} \qquad C_{l_{\delta_r}} = \frac{\partial C_l}{\partial \delta_r} \qquad C_{l_{\delta_s}} = \frac{\partial C_l}{\partial \delta_s}$$

$$C_{m_{\delta_{f3}}} = \frac{\partial C_m}{\partial \delta_{f3}} \qquad C_{m_q} = \frac{\partial C_m}{\partial \frac{q\bar{c}}{2V}} \qquad C_{m_{\dot{\alpha}}} = \frac{\partial C_m}{\partial \frac{\dot{\alpha}\bar{c}}{2V}}$$

$$C_{m_{\delta_s}} = \frac{\partial C_m}{\partial \delta_s} \qquad C_{m_{\delta_{sp}}} = \frac{\partial C_m}{\partial \delta_{sp}} \qquad C_{m_{\delta_t}} = \frac{\partial C_m}{\partial \delta_t}$$

$$C_{n_p} = \frac{\partial C_n}{\partial \frac{pb}{2V}} \qquad C_{n_r} = \frac{\partial C_n}{\partial \frac{rb}{2V}} \qquad C_{n_\beta} = \frac{\partial C_n}{\partial \beta}$$

$$C_{n_{\delta_a}} = \frac{\partial C_n}{\partial \delta_a} \qquad C_{n_{\delta_r}} = \frac{\partial C_n}{\partial \delta_r} \qquad C_{n_{\delta_s}} = \frac{\partial C_n}{\partial \delta_s}$$

$$C_{X_{\delta_s}} = \frac{\partial C_X}{\partial \delta_s} \qquad C_{X_{\delta_{sp}}} = \frac{\partial C_X}{\partial \delta_{sp}} \qquad C_{X_{\delta_t}} = \frac{\partial C_Z}{\partial \delta_t}$$

$$C_{Y_p} = \frac{\partial C_Y}{\partial \frac{pb}{2V}} \qquad C_{Y_r} = \frac{\partial C_Y}{\partial \frac{rb}{2V}} \qquad C_{Y_\beta} = \frac{\partial C_Y}{\partial \beta}$$

$$C_{Y_{\delta_a}} = \frac{\partial C_Y}{\partial \delta_a} \qquad C_{Y_{\delta_r}} = \frac{\partial C_Y}{\partial \delta_r} \qquad C_{Y_{\delta_s}} = \frac{\partial C_Y}{\partial \delta_s}$$

$$C_{Z_{\delta_s}} = \frac{\partial C_Z}{\partial \delta_s} \qquad C_{Z_{\delta_{sp}}} = \frac{\partial C_Z}{\partial \delta_{sp}} \qquad C_{Z_{\delta_t}} = \frac{\partial C_Z}{\partial \delta_t}$$

Abbreviations:

ADI	attitude director instrument
BLC	boundary-layer control
CTOL	conventional take-off and landing
DLC	direct lift control
DME	distance measuring equipment

EBF	externally blown flap
HSI	horizontal situation indicator
IFR	Instrument Flight Rules
ILS	instrument landing system
OASPL	overall sound pressure level
PR	pilot rating
SPL	sound pressure level
STOL	short take-off and landing
VFR	Visual Flight Rules
VOR	visual omnirange

DESCRIPTION OF SIMULATED AIRPLANE

The STOL airplane design used in this study was a four-engine subsonic jet transport with a high wing and high-bypass-ratio turbofan engines. A three-view drawing of the configuration is presented in figure 1, and a detailed description of the aerodynamic data for the configuration is given in reference 2. The engines were mounted in such a manner that the jet exhaust impinged directly on the trailing-edge flap system (fig. 1(b)), and the design is referred to as an externally blown flap (EBF) configuration.

The static aerodynamic data used from reference 2 represent the condition of blowing over the wing leading edge and the rudder (BLC). The major effect of blowing over the wing was to increase the stall angle of attack, particularly for the lower engine-thrust conditions. Blowing on the rudder more than doubled the basic rudder effectiveness.

The simulated airplane had a gross weight of 245 kN (55 100 lbf), a wing loading of 3131 N/m^2 (65.4 lbf/ft^2), and a thrust-weight ratio of 0.60 for the maximum thrust condition. The mass and dimensional characteristics of the airplane are presented in table I, and the aerodynamic characteristics are presented in table II. The maximum control-surface deflection and deflection rates are also presented in table I. Note that the flap deflection was limited to 35^o to 70^o – the range for which force-test data were available.

The airplane was augmented longitudinally with a pitch attitude command system and an autospeed system as described in reference 1. The only modification made for the present study was that the commanded velocity of the autospeed system was scheduled to give desired deceleration rates. This airspeed scheduling was activated by a switch located in the center console of the cockpit.

Symmetrical spoiler deflections were used for direct lift control (DLC).

DESCRIPTION OF SIMULATION EQUIPMENT

The fixed-base simulator had a transport-type cockpit which was equipped with conventional flight and engine-thrust controls and with a flight-instrument display panel representative of those found in current transport airplanes. (See fig. 2.) In addition, a direct lift controller (DLC) was available. (An instrument was installed in the display panel to indicate the amount of DLC being commanded.) Instruments indicating angle of attack, sideslip, and flap deflection were also provided. A conventional cross-pointer-type flight director instrument was used, but the command bars (cross pointers) were driven by the main computer program. (See ref. 1 for a detailed description of the flight director system used in this study.) A feature of the attitude director instrument (ADI) which was used in the present study but not used or discussed in reference 1 was the Fast/Slow feature of this instrument. During the present investigation the Fast/Slow indicator (fig. 2) was used to provide the pilot with information regarding the airspeed of the aircraft as compared to the desired airspeed.

The simulator control forces were provided by a hydraulic servosystem and were functions of control displacement and rate. The control characteristics of the simulator are defined in table III. Real-time digital simulation techniques were used wherein a digital computer was programed with equations of motion for six degrees of freedom. The simulator did not incorporate cockpit motion; a visual display of a hypothetical STOL airport was used.

TESTS AND PROCEDURES

The ILS approach was initiated with the airplane in the power-approach condition (power for level flight) at an altitude below the glide slope, and at a variable distance from the runway. (The distance from the runway and the altitude varied with glide-slope angle and/or the planned deceleration rate.) Various piloting techniques were developed for performing decelerating approaches on 6° and 7.5° glide slopes.

The pilot's task was to capture the localizer and the glide slope and to maintain them as closely as possible while decelerating from an initial airspeed of 140 knots to a final airspeed of 75 knots under IFR conditions. (Although the visual display was available and some landings were made, the approach was usually terminated after the deceleration task was completed.) Two NASA research pilots used various piloting techniques and rates of deceleration in order to determine: (1) the most effective technique from a piloting standpoint; (2) the limitations of the airplane configuration with regard to the maximum attainable deceleration rate for each piloting technique; and (3) the effects of the various piloting techniques and deceleration rates on the ground noise levels that may be expected.

RESULTS AND DISCUSSION

The results of this investigation are discussed in terms of the previously stated objectives. Also, throughout the discussion, the pilot ratings listed apply to the deceleration tasks since the handling qualities of the fully augmented airplane were assigned a pilot rating of 2 for the constant speed (V = 75 knots or 140 knots) landing approach task. (See table IV for pilot rating system.) Since there were little differences in pilot performance, and therefore pilot rating, for glide-slope angles of 6° or 7.5°, all results discussed pertain to a glide-slope angle of 7.5°.

Maximum Rate of Descent

In order to realize the greatest benefits from performing decelerating approaches, the deceleration should be made as late as possible during the landing approach. This, of course, presents the problem of unusually high rates of descent near the ground – particularly for steep approaches. The question quite naturally arises then as to the maximum rate of descent that the pilot will tolerate prior to the flare.

There are many documented tests suggesting a limiting value on acceptable rate of descent near the ground – the most often quoted value being 305 m/min (1000 ft/min). For example, reference 5 states that even for VFR conditions, when below an altitude of about 61 m (200 ft), the time available for making decisions becomes too short and the judgment required to execute the flare properly becomes excessive for rates of descent greater than 305 m/min (1000 ft/min).

In order to define the minimum altitude at which the deceleration must be completed, tests were made early in the study to determine the minimum altitude for which the pilots would accept a rate of descent as high as 305 m/min (1000 ft/min). (For a glide slope of 7.5° and an airspeed of 75 knots, the rate of descent is 302 m/min (992 ft/min).) Following these tests, the pilots concluded that, although this STOL configuration had very good flight-path response throughout the test airspeed range (V = 140 to 75 knots), they would

not accept a rate of descent higher than 305 m/min (1000 ft/min) below an altitude of 152 m (500 ft). This result therefore dictated that when flying a 7.5° glide slope, the deceleration from 140 knots to 75 knots should be completed at an altitude greater than 152 m (500 ft). It can be seen from figure 3 that the deceleration procedures used in the present study satisfy the requirements of reference 5; and furthermore, if a two-segment approach ($7.5^{\circ}/4^{\circ}$) is used, the rate of descent from which this STOL airplane is flared will be equal to or less than the rate of descent of current jet transports.

The ability to make the transition to a second glide-slope segment or the capability to flare this EBF airplane will not be discussed in this paper since they were discussed in detail in reference 1. The results of the present investigation are discussed in terms of the deceleration procedures – the flight was considered to be terminated after the deceleration had been completed.

Deceleration Techniques

Throughout this study various techniques were used to perform the decelerating approach, but in each instance the approach was initiated at $V = 140$ knots and was completed at $V = 75$ knots. The altitude at which the deceleration was completed was usually near 152 m (500 ft), but, of course, the altitude at which the deceleration was initiated depended upon the desired deceleration rate.

Technique 1.- Piloting technique 1 consisted of a manual deceleration (autospeed system initially inactive) to an airspeed of 75 knots. Once $V = 75$ knots was attained, the autospeed system was activated and airspeed was held at 75 knots, automatically, for the remainder of the flight.

The initial conditions of the various flights made using deceleration technique 1 were always the same with the exception of altitude, which was varied as the desired deceleration rate varied. The initial conditions used when a deceleration rate of 0.30 m/sec^2 (1 ft/sec^2) was to be commanded were: $h = 1219$ m (4000 ft); $V = 140$ knots; $\gamma = 0^{\circ}$; $\theta = -5^{\circ}$; $\delta_{f3} = 40^{\circ}$; and $\delta_{sp} = 0^{\circ}$. To capture the 7.5° glide slope, the pilot moved δ_{sp} to approximately 35° while adjusting θ and the thrust (T) to attain a glide slope of 7.5° and to maintain an airspeed of 140 knots. (See fig. 4.) At an altitude of approximately 1006 m (3300 ft), the copilot initiated the deceleration schedule with a switch provided on the center console. Activation of this switch initiated the velocity scheduling to provide a given deceleration rate; this information was then used to drive the Fast/Slow indicator on the ADI. By continuously adjusting θ and T, the pilot attempted to maintain glide slope with the aid of the horizontal bar of the flight director (fig. 2), and to maintain the proper deceleration rate with the aid of the Fast/Slow indication of the ADI. After an airspeed of approximately 105 knots was attained, the copilot moved the flaps from 40° to 55° in an attempt to keep the angle of attack as low as possible and thus maintain an

adequate safety margin from the stall. At an airspeed of 75 knots, the autospeed was automatically engaged and the pilot reverted to the direct-lift controller (DLC) for glide-path control. The pilot could then either flare and land the airplane from the 7.5^{o} glide slope or make the transition to a more shallow glide slope (4^{o}) and land.

Typical time histories of the motions obtained when using technique 1 for decelerating from V = 140 knots to 75 knots are shown in figure 4. Figure 4(a) is for a deceleration rate of 0.30 m/sec^2 (1 ft/sec^2). The pilot commented that although he was quite busy during the deceleration portion of the approach, the task was not too difficult and he assigned a pilot rating of 3.5 to the deceleration task. Figure 4(b) presents a time history for a deceleration rate of 0.61 m/sec^2 (2 ft/sec^2). The pilot assigned a rating of 4.5 to this deceleration task, his comment being that all errors (ϵ_{zh} and $\dot{V}$) were larger for the higher rate of deceleration. (These points are apparent when comparing ϵ_{zh} and $\dot{V}$ in figs. 4(a) and 4(b).) For a commanded deceleration rate of 0.91 m/sec^2 (3 ft/sec^2), figure 4(c), the pilot assigned a rating of 7 to the deceleration task with the comments that, (1) the changes required in thrust were too large and too fast, and (2) in order to achieve the commanded deceleration rate, the angle of attack required was too close to the stall angle of attack ($\alpha_{stall} \approx 25^{o}$). (Note that the pilot had to use symmetrical spoilers (δ_{sp}) as well as thrust to maintain glide slope for the time history shown in fig. 4(c).) For commanded rates of deceleration of 1.22 m/sec^2 (4 ft/sec^2) and higher, the pilot assigned a rating of 10 to the deceleration task with the comment that the variables were changing too rapidly for him to maintain adequate control.

Technique 2.- The second technique of flying the decelerating approach differed from technique 1 in that for technique 2, the airspeed was automated throughout the approach and landing, and the thrust remained constant. (The autospeed system drove the third segment flap (δ_{f3}) to maintain a selected airspeed schedule.) When using technique 2, the pilot employed his DLC (symmetrical spoilers) to capture and track the glide slope, as well as to perform the landing flare. After the copilot initiated the deceleration schedule, the pilot only had to monitor the horizontal bar of the flight director to maintain glide slope. (He did not have to monitor the Fast/Slow indicator for this deceleration technique since maintenance of the airspeed schedule was automated.) At an airspeed of approximately 130 knots, the pilot began to pitch the airplane slowly from its nosedown attitude ($\theta = -5^{o}$) to the desired landing attitude ($\theta \approx +5^{o}$), attempting to reach $\theta \approx +5^{o}$ by the time the airspeed had decreased to approximately 100 knots.

The pilots assigned a rating of 1.5 to the deceleration task when technique 2 was used, and commented that the task was very easy for any deceleration rate commanded. (Commanded deceleration rates from 0.30 m/sec^2 (1 ft/sec^2) to 3.05 m/sec^2 (10 ft/sec^2) were flown.) Although the higher commanded deceleration rates ($\dot{V} > 1.52$ m/sec^2 (5 ft/sec^2)) did not affect the pilot's ability to perform the deceleration task, and there-

fore did not affect the pilot rating, the speed controller (δ_{f3}) became limited for a longer period of time as the command $\dot{V}$ was increased. Typical time histories are presented in figure 5 for which technique 2 was used for various rates of deceleration.

Figure 5(a) is a time history of the results obtained when a deceleration rate of 0.30 m/sec^2 (1 ft/sec^2) was commanded. As seen from the time history of $\dot{V}$, the rate of deceleration was very smooth. Figure 5(b) represents the case for which a deceleration rate of 1.52 m/sec^2 (5 ft/sec^2) was commanded. The deceleration was still performed smoothly; however, the time history of the speed controller (δ_{f3}) shows that the flaps almost reached their maximum deflection limit of 70°. As stated previously, the flaps reached this deflection limit for commanded deceleration rates higher than 1.52 m/sec^2 (5 ft/sec^2). The results obtained when the flap limits occurred are illustrated in figure 5(c), which represents the results obtained when the commanded deceleration rate was 2.44 m/sec^2 (8 ft/sec^2). Note that this commanded rate could not be maintained once the flaps (δ_{f3}) became limited. Figures 5(c) and 5(d) indicate that the greater the deceleration rate commanded, the longer the period of time δ_{f3} remained limited.

Technique 3.- Technique 3 differed from technique 1 in that the airspeed schedule was automated. Also, technique 3 differed from technique 2 in that thrust (as opposed to spoiler DLC) was used to track the glide slope during the period of deceleration.

When using technique 3, the pilot captured the 7.5° glide slope with the spoilers (δ_{sp}). After stabilizing on the glide slope, the pilot set δ_{sp} at about 35° (the amount required to flare and land from a glide slope of 7.5°) and then tracked the glide slope with the throttles (thrust modulation) during the deceleration period. At an airspeed of approximately 130 knots, the pilot began to pitch the airplane slowly from its nosedown attitude ($\theta \approx -5°$) to the desired landing attitude ($\theta \approx +5°$), attempting to reach $\theta = +5°$ by the time the airspeed had decreased to approximately 100 knots. Following completion of the deceleration (V = 75 knots at h ≈ 152 m (500 ft)), the pilot used DLC (spoiler modulation) to flare and land the airplane.

The pilots assigned a rating of 2 to the deceleration task when technique 3 was used, and commented that the task was very easy for any deceleration rate commanded. Also, the pilots commented that although the flight-path response to thrust inputs was quite adequate, the response was not as rapid or precise as when spoiler DLC (technique 2) was used to track glide slope. Similar to technique 2, it was found that although the pilot rating did not vary with various commanded deceleration rates, the flaps reached the limit of 70° for commanded deceleration rates higher than 1.52 m/sec^2 (5 ft/sec^2). Typical time histories for which technique 3 was used to decelerate from 140 knots to 75 knots are presented in figures 6(a), 6(b), and 6(c), which represent commanded deceleration rates of 0.61, 1.83, and 3.05 m/sec^2 (2, 6, and 10 ft/sec^2), respectively.

Technique 4.- The fourth technique of performing the deceleration task was designed to minimize the thrust required to "fly" a 7.5° landing approach in an effort to decrease the noise level of the aircraft in the terminal area. The initial conditions used for technique 4 were: V = 140 knots; $\gamma = 0^{\circ}$; $\theta = -2^{\circ}$; $\delta_{f3} = 36^{\circ}$; and $\delta_{sp} = 10^{\circ}$. To capture the glide slope, the pilot pitched over to approximately -10° while adjusting thrust to attain and maintain a glide slope of 7.5°. (Airspeed was automated throughout the flight.) The copilot initiated the deceleration at the desired altitude and the pilot tracked the glide slope with thrust modulation (throttles). As soon as the deceleration was initiated, the spoilers were automatically closed according to a schedule such that zero deflection was reached at V = 90 knots. Also, upon reaching 115 knots the airplane was slowly pitched up (automatically) from a nosedown attitude of -10° to approximately $+5^{\circ}$ so that this desired landing attitude was attained by the time the deceleration was completed; V = 75 knots and $h \approx 152$ m (500 ft). From this condition, the pilot could either flare and land the airplane from the 7.5° glide slope or make the transition to a more shallow glide slope (4°) and land – still using thrust modulation to control rate of sink.

The pilots assigned a rating of 3 to technique 4 for all deceleration rates commanded. Although the pilots assigned a "satisfactory" rating to this deceleration technique, they had two objections to the technique. One objection concerned the thrust response, which they characterized as not being sufficiently fast or precise enough at the lower engine rpm. It can be seen from figure 7 that for all deceleration rates commanded, the thrust required to maintain glide slope approached the "idle" value (T = 6.7 kN) at an airspeed of approximately 90 knots. The other objection to this technique concerned the automation of the pitch attitude change, as well as the rate at which the system pitched the aircraft. The pilots said that they were concerned whether the automated pitch schedule was going to perform correctly.

Typical time histories of decelerating approaches made using technique 4 are presented in figure 7. Figures 7(a), 7(b), 7(c), and 7(d) represent commanded deceleration rates of 0.30, 0.61, 0.91, and 1.22 m/sec^2 (1, 2, 3, and 4 ft/sec^2), respectively. It should be noted that although these aforementioned deceleration rates were "commanded," they could not be maintained throughout the deceleration period, with the exception of that shown in figure 7(a), due to the flaps reaching the 70° limit. (See $\dot{V}$ and δ_{f3} in figs. 7(a) to 7(d).) Also note, however, that although the flaps became limited for the commanded deceleration rate of 0.61 m/sec^2 (2 ft/sec^2), the time required for the deceleration is reduced from 118 seconds for a "commanded" $\dot{V}$ of -0.30 m/sec^2 (-1 ft/sec^2) to 63 seconds for a "commanded" $\dot{V}$ of -0.61 m/sec^2 (-2 ft/sec^2). It is therefore concluded from figures 7(a) and 7(b) that using a commanded $\dot{V}$ of -0.61 m/sec^2 (-2 ft/sec^2) would be beneficial from a "time required to decelerate" standpoint; however, when a deceleration rate greater than about 0.61 m/sec^2 (2 ft/sec^2) is commanded, the additional

benefits are small. (The times required to complete the decelerations shown in figs. 7(c) and 7(d) were 50 seconds and 48 seconds, respectively.)

The benefits realized by using this technique from a ground-noise standpoint will be discussed later in this report.

Effects of Deceleration Techniques and Rates on Approach Time

One obvious advantage of the decelerating approach over the constant slow-speed approach (V = 75 knots) is the lesser amount of time required to fly the final approach. From a traffic scheduling and control viewpoint, this feature is highly desirable. Table V presents the total amount of time required to attain an altitude of 152 m (500 ft), starting from h = 1219 m (4000 ft), for typical 7.5° approaches. (The amount of time required for this portion of the approach when flying at a constant speed of 75 knots was 212 seconds.)

Table V indicates that for piloting technique 1 and a deceleration rate of 0.91 m/sec^2 (3 ft/sec^2) the total time required was 121 seconds, which was a reduction of 91 seconds over a constant speed (V = 75 knots) approach. This value represents a substantial reduction in time, but it must be noted that this deceleration technique and rate were assigned a pilot rating of 7, which represents an unacceptable task. It is also shown that the approach with a deceleration rate of 0.61 m/sec^2 (2 ft/sec^2) represents an acceptable task (PR = 4.5) and a time reduction of 82 seconds. From these two results, it can be concluded that when using piloting technique 1, the maximum deceleration that should be attempted is approximately 0.61 m/sec^2 (2 ft/sec^2).

For piloting techniques 2 and 3, the pilot ratings were 1.5 and 2, respectively, for "commanded" deceleration rates as high as 3.05 m/sec^2 (10 ft/sec^2). However, it is apparent from table V that deceleration rates greater than approximately 1.22 m/sec^2 (4 ft/sec^2) represent essentially no additional savings in approach time. This effect is primarily due to the speed controller (δ_{f3}) becoming limited for the higher commanded deceleration rates; therefore, it is concluded that for techniques 2 and 3, the maximum deceleration rate that can usefully be commanded is approximately 1.22 m/sec^2 (4 ft/sec^2).

Similarly, when using piloting technique 4, the "minimum noise" technique, the flaps become limited for commanded deceleration rates greater than about 0.61 m/sec^2 (2 ft/sec^2) and therefore little or no reduction in the final approach time is realized – a deceleration rate greater than approximately 0.61 m/sec^2 (2 ft/sec^2) need not be commanded. (See fig. 7.)

Effects of Winds on Deceleration Techniques

Various atmospheric conditions were simulated, including steady winds, wind shears, and turbulence, to determine the effects, if any, on the previously discussed piloting techniques.

The various steady winds simulated included head winds as high as 25 knots and tail winds as high as 10 knots. The wind shears simulated were as high as 8 knots per 30 m (100 ft) of altitude. The turbulence model used in this simulation was a modified version of the Dryden model and included scale lengths of 183 m (600 ft) for the longitudinal and lateral turbulence, and 9 m (30 ft) for the vertical turbulence. The root-mean-square gust intensities used for the longitudinal, lateral, and vertical turbulence were 2.5, 1.6, and 1.5 knots, respectively.

The various steady winds and wind shears that were simulated were found to affect the altitude at which the deceleration should be initiated in order to complete the deceleration at $h \approx 152$ m (500 ft), but this was essentially the only effect noticed by the pilots. The pilot ratings assigned to the various decelerating techniques and deceleration rates remained the same when the steady winds and wind shears were present as when they were not simulated.

When atmospheric turbulence was simulated, the pilot ratings assigned to the various decelerating techniques and deceleration rates were all increased by one-half pilot rating because of the increase in pilot workload required to track the glide slope and the localizer in turbulence. The level of turbulence simulated had little effect on the ability to affect the deceleration, whether it was done manually or by the automatic system.

Ride Qualities

The question naturally arises as to what effect the previously discussed piloting techniques have on the ride qualities of the subject STOL airplane. Very little data are available on subjective response to motion in the longitudinal direction, and the wide variation in both magnitudes and trends reported by various researchers requires a conservative approach to any criteria suggested to date. For example, reference 6 states that if the maximum accelerations exceed 3.0 m/sec^2 (10 ft/sec^2), passengers may be expected to complain, whereas reference 7 suggests that the "maximum allowable" value of longitudinal acceleration or deceleration be 0.13g.

Considering the maximum values of deceleration rates suggested previously, it can be seen from table V that the corresponding levels of longitudinal deceleration fall within the more conservative (0.13g) ride-quality criterion. It is therefore concluded that the deceleration procedures investigated in this study should be acceptable from a passenger comfort standpoint.

Curved-Descending Instrument Approaches

In order to reduce the congestion caused by long straight-in approaches which are required for CTOL transport operations, curved, steep descending flight paths may be required of future STOL transports if they are to operate into high-density airports

(fig. 8). Accordingly, a brief attempt was made during the present study to determine if a curved-descending approach, as opposed to the previously discussed straight-in approach, would have adverse effects on the deceleration techniques developed.

Since the curved-descending approach was not considered to be a major objective of this study, the advanced flight instrumentation that would probably be used for such maneuvers was not developed. The basic instrumentation used for this brief portion of the study consisted of the conventional flight director system which included an attitude director indicator (ADI) and a horizontal situation indicator (HSI) with DME (distance-measuring equipment) and course heading windows. The commanded course for this HSI was not continuously updated during the descending turn; therefore, the major instrument used by the pilot for tracking the curved portion of the approach was the DME. (The DME used in this simulation showed the pilot the distance of the aircraft from the VOR (DME) station with an instrument resolution of 0.1 nautical mile.)

All curved-descending approaches were made in still air – no winds or turbulence were included.

The ground projection of the curved approach path used in this simulation is presented in figure 9. The aircraft was trimmed for straight and level flight (V = 140 knots, h = 1312 m (4300 ft), heading of 180^{o}) at point A. As the aircraft neared point B, the pilot established a rate of sink of 518 m/min (1700 ft/min) and banked the aircraft approximately 11^{o} to initiate the desired turn at a turn radius of 1.5 nautical miles. The pilot maintained the proper ground track (turn radius) by utilizing the DME information. After the aircraft passed through point C, the ILS glide slope was acquired; instead of the steady rate of descent, the pilot used the ILS glide-slope information to capture and maintain 7.5^{o}. For a commanded deceleration rate of 0.61 m/sec^2 (2 ft/sec^2), the copilot initiated the deceleration at point D; $h \approx 550$ m (1800 ft). As the aircraft flew through point E, the ILS localizer was acquired, and from this point the pilot disregarded the DME information and "flew" using the ILS localizer and glide slope through point F. (For curved-descending approaches, the ILS localizer beam was considered to be 10^{o} ($\pm 5^{o}$) wide, instead of the conventional 5^{o} ($\pm 2.5^{o}$) wide.) Point F denotes the general location of the aircraft at which the deceleration was completed.

It was determined that making such curved-descending approaches had no significant effects on the previously discussed deceleration techniques. When using technique 2, for example, the pilot assigned a rating of 3.0 to the approach task for all deceleration rates. (A pilot rating of 1.5 was assigned to the deceleration task for straight-in approaches when technique 2 was used.) The reason for the higher pilot rating when making the curved approach was the increase in pilot workload in the lateral axis, a factor which could be alleviated with the proper flight instrumentation, such as a more sophisticated flight director and/or a pictorial display.

Curved-descending approaches were also made where the turn radius was 0.75 nautical mile, and the pilot rating increased by 0.5 with the comment that it became more difficult to "fly" the DME because of the higher accuracy required for bank-angle control.

Noise Considerations

Most of the landing approach noise abatement research has been concentrated on the use of modified profiles (steep and/or two segment). However, decelerating landing approaches are another means of reducing noise. The decelerating technique can be combined with normal, steep, or various two-segment profiles, but the majority of any noise reduction realized will, to a great extent, depend on the amount of engine-thrust reduction used during the decelerating period.

During the present simulation program, calculations were made of the overall sound pressure level (OASPL) at a point on the ground directly beneath the aircraft in order to allow comparisons of various piloting techniques and deceleration rates from a noise viewpoint. Incremental differences in computed noise levels between two flights provided a measure of how "noisy" one is with respect to the other. That is,

$$\Delta OASPL = OASPL_i - OASPL_R$$

where the subscript i refers to the flight under investigation and the subcript R refers to the reference flight. The sound pressure level was calculated as a function of four variables: (1) engine thrust; (2) distance between the airplane and a hypothetical ground station always located directly beneath the aircraft; (3) angle between the airplane engine axis and the ground-station line of sight; and (4) flap deflection.

Noise data for the basic TF-34 engine were obtained from the engine manufacturer. The data provided a reference overall sound pressure level (SPL) as a function of the variables (1), (2), and (3) listed in the preceding paragraph. (Extrapolation to the actual range was accomplished by using the basic spherical wave relationship that intensity is inversely proportional to the square of the range.) In addition, a factor was added to account for noise due to jet exhaust interaction with the flaps. Because of the lack of measured data, this "flap scrub" noise was roughly approximated to be linear with flap deflection, and a value of 0.167 dB/deg was used.

All flights were initiated below the 7.5^{o} glide slope at an altitude of 1219 m (4000 ft) and an airspeed of 140 knots; then the glide slope was secured and the deceleration to 75 knots was performed. The factors examined were (1) the effect of the deceleration technique, and (2) the effect of the deceleration rate.

Figure 10 presents the calculated values of the overall sound pressure level for the previously discussed deceleration techniques as compared with constant airspeed

(V = 75 knots) landing approaches. It can be concluded from figure 10 that, in general, any of the deceleration techniques used during this study tend to have a favorable effect on the absolute ground noise level (OASPL) over that of the constant speed (V = 75 knots) landing approach. It should also be mentioned that, in addition to the lower OASPL values realized by flying a decelerating approach, the amount of time that an individual located at a given point along the approach path would be exposed to the noise level would be less than when the aircraft is flown at a slower-constant airspeed (V = 75 knots).

Figure 11 presents a comparison of ground noise levels produced by the various deceleration techniques; that is, the noise levels for the various techniques are compared to each other for the same deceleration rate (0.30 m/sec^2 (1 ft/sec^2)). Figure 11(a) shows that, in general, technique 1 would produce less noise than techniques 2 and 3, and figure 11(d) indicates that technique 4 would tend to be less noisy than any of the other three techniques.

An attempt was made to determine the effect of the rate of deceleration on the ground noise produced. The results indicated that the higher deceleration rates afford no obvious advantage over the lower rate in the OASPL reduction. Subjectively, however, the higher rates may be more desirable simply because of lower exposure time to the noise.

SUMMARY OF RESULTS

A fixed-base simulator program was conducted to define the problems and methods of solution associated with performing decelerating landing approaches on a representative STOL transport, equipped with an external-flow jet flap in combination with high-bypass-ratio fan-jet engines.

Four piloting techniques were developed for performing the decelerating approach. These were as follows:

1. A manual deceleration for which the pilot tracked the glide slope and "flew" the commanded airspeed schedule with a combination of pitch attitude and thrust.

2. The pilot tracked glide slope with a direct-lift controller (DLC) that consisted of symmetrical spoiler modulation. The desired airspeed schedule was maintained by an automatic speed controller.

3. The pilot tracked glide slope with throttles (thrust modulation). The desired airspeed schedule was maintained automatically.

4. The pilot tracked glide slope with throttles, after he had pitched the aircraft to -10° to capture the glide slope. The desired airspeed schedule was maintained automatically.

The deceleration rates simulated varied from 0.30 m/sec^2 (1 ft/sec^2) to 3.05 m/sec^2 (10 ft/sec^2).

The results of this simulation program may be summarized as follows:

1. Although this STOL configuration had very good flight-path response throughout the test airspeed range (V = 140 to 75 knots), the pilots would not accept a rate of descent higher than 305 m/min (1000 ft/min) at altitudes below 152 m (500 ft). Accordingly, when flying a 7.5^o glide slope, the deceleration to 75 knots should be completed at an altitude no less than 152 m (500 ft).

2. For piloting technique 1 (the manual deceleration) the pilots assigned an unacceptable rating to the deceleration task for deceleration rates greater than 0.61 m/sec^2 (2 ft/sec^2). For higher rates of deceleration, the pilot thrust inputs required were too large and too fast, and the angle of attack required was too close to the stall angle of attack to achieve the commanded deceleration rate and maintain the 7.5^o glide slope.

3. For piloting techniques 2 and 3, the pilots assigned satisfactory ratings to the deceleration task for any deceleration rate commanded. (Commanded deceleration rates from 0.30 m/sec^2 (1 ft/sec^2) to 3.05 m/sec^2 (10 ft/sec^2) were flown.) Although the relatively high commanded deceleration rates did not affect the pilot's ability to perform the deceleration task, and therefore did not affect the pilot rating, the automatic speed controller (δ_{f3}) became limited for commanded deceleration rates greater than 1.52 m/sec^2 (5 ft/sec^2). Thus, sustained deceleration rates greater than 1.52 m/sec^2 (5 ft/sec^2) could not be attained.

4. The pilots assigned a satisfactory rating to technique 4 for all deceleration rates commanded. However, sustained deceleration rates greater than approximately 0.61 m/sec^2 (2 ft/sec^2) could not be attained.

5. When a decelerating approach was made the amount of time required to attain an altitude of 152 m (500 ft), starting from an altitude of 1219 m (4000 ft), was found to be as much as 1.5 minutes less than the amount of time required for a constant 75-knot approach speed.

6. The simulated steady winds, wind shears, or turbulence had little effect on the pilots' ability to perform the deceleration, whether it was done manually or by the automatic system.

7. The deceleration procedures suggested in this study should be acceptable from a passenger comfort standpoint.

8. The curved-descending approaches flown had no significant effects on the deceleration procedures investigated.

9. Decelerating landing approaches are another means of reducing the ground noise level. Indications are that, in general, technique 1 would produce less noise than techniques 2 and 3, and technique 4 would tend to be less noisy than any of the other three techniques.

Langley Research Center,
National Aeronautics and Space Administration,
Hampton, Va., January 2, 1974.

REFERENCES

1. Grantham, William D.; Nguyen, Luat T.; Patton, James M., Jr.; Deal, Perry L.; Champine, Robert A.; and Carter, C. Robert: Fixed-Base Simulator Study of an Externally Blown Flap STOL Transport Airplane During Approach and Landing. NASA TN D-6898, 1972.

2. Parlett, Lysle P.; Greer, H. Douglas; Henderson, Robert L.; and Carter, C. Robert: Wind-Tunnel Investigation of an External-Flow Jet-Flap Transport Configuration Having Full-Span Triple-Slotted Flaps. NASA TN D-6391, 1971.

3. Grafton, Sue B.; Parlett, Lysle P.; and Smith, Charles C., Jr.: Dynamic Stability Derivatives of a Jet Transport Configuration With High Thrust-Weight Ratio and an Externally Blown Jet Flap. NASA TN D-6440, 1971.

4. Vogler, Raymond D.: Wind-Tunnel Investigation of a Four-Engine Externally Blowing Jet-Flap STOL Airplane Model. NASA TN D-7034, 1970.

5. Innis, Robert C.; Holzhauser, Curt A.; and Quigley, Hervey C.: Airworthiness Considerations for STOL Aircraft. NASA TN D-5594, 1970.

6. McFarland, Ross Armstrong: Human Factors in Air Transportation: Occupational Health and Safety. First ed., McGraw-Hill Book Co., Inc., 1953.

7. Jacobson, Ira D.: Criteria for Ride Quality – Motion. STOL Prog. Mem. Rep. 40302, Univ. of Virginia, Center Appl. Sci. & Eng. Public Aff., Feb. 1972.

TABLE I.- MASS AND DIMENSIONAL CHARACTERISTICS

Weight, N (lbf)	245 096	(55 100)
Wing area, m^2 (ft^2)	78	(843)
Wing span, m (ft)	24	(78)
Mean aerodynamic chord, m (ft)	3.58	(11.74)
Center-of-gravity location, percent $\bar{c}$		40
I_X, kg-m^2 (slug-ft^2)	331 103	(244 212)
I_Y, kg-m^2 (slug-ft^2)	334 637	(246 819)
I_Z, kg-m^2 (slug-ft^2)	625 677	(461 482)
I_{XZ}, kg-m^2 (slug-ft^2)	27 690	(20 423)
Maximum control-surface deflections:		
δ_t, deg		±15
δ_{f3}, deg		35 to 70
δ_{sp}, deg		0 to 60
δ_s, deg		±60
δ_a, deg		±20
δ_r, deg		±40
Maximum control-surface deflection rates:		
$\dot{\delta}_t$, deg/sec		50
$\dot{\delta}_{f3}$, deg/sec		5
$\dot{\delta}_{sp}$, deg/sec		50
$\dot{\delta}_s$, deg/sec		50
$\dot{\delta}_a$, deg/sec		50
$\dot{\delta}_r$, deg/sec		50

TABLE II.- BASIC AERODYNAMIC INPUTS USED IN SIMULATION

α, deg	C_T=0	C_T=1.87	C_T=3.74	C_T=0	C_T=1.87	C_T=3.74	C_T=0	C_T=1.87	C_T=3.74	C_T=0	C_T=1.87	C_T=3.74
	C_m			$C_{m_{\delta_{f3}}}$, per deg			C_{m_q}, per rad			$C_{m_{\dot{\alpha}}}$, per rad		
-10	0.81	0.15	-0.28	-0.0001	0.0016	-0.0036	-28.60	-17.86	-28.60	-11.40	-7.14	-11.40
-5	.41	-.03	-.36	.0006	.0021	-.0023	-28.60	-26.80	-28.60	-11.40	-10.70	-11.40
0	.04	-.23	-.47	.0013	.0026	-.0010	-28.60	-32.15	-29.30	-11.40	-12.85	-11.70
5	-.25	-.38	-.60	.0019	.0022	0	-26.45	-34.30	-30.00	-10.55	-13.70	-12.00
10	-.34	-.57	-.70	.0019	.0034	.0003	-21.44	-32.86	-30.36	-8.56	-13.14	-12.14
15	-.47	-.63	-.81	.0033	.0030	.0005	-10.72	-30.72	-31.45	-4.28	-12.28	-12.55
20	-.43	-.62	-.81	.0026	.0020	-.0005	-3.57	-30.00	-31.45	-1.43	-12.00	-12.55
25	-.48	-.59	-.81	.0030	.0016	-.0004	-5.00	-28.60	-30.36	-2.00	-11.40	-12.14
30	-.45	-.65	-.71	.0022	.0042	-.0006	-9.29	-39.30	-48.60	-3.71	-15.70	-19.40
	$C_{X_{\delta_s}}$, per deg			$C_{Z_{\delta_s}}$, per deg			$C_{m_{\delta_s}}$, per deg			$C_{Y_{\delta_s}}$, per deg		
-10	-0.0012	-0.0024	-0.0026	0.0093	0.0140	0.0148	-0.0012	0.0006	0.0052	-0.0002	0	0.0002
-5	-.0016	-.0016	-.0028	.0105	.0165	.0161	-.0017	-.0007	.0025	-.0002	-.0001	.0002
0	-.0020	-.0008	-.0030	.0117	.0192	.0173	-.0022	-.0020	-.0002	-.0002	-.0002	0
5	-.0026	-.0013	-.0032	.0128	.0209	.0173	-.0008	-.0022	-.0017	-.0002	-.0002	-.0001
10	-.0033	-.0021	-.0028	.0119	.0217	.0185	-.0002	-.0020	-.0020	-.0003	-.0003	-.0002
15	-.0035	-.0033	-.0046	.0099	.0219	.0186	.0008	-.0012	-.0012	-.0002	-.0003	-.0002
20	-.0028	-.0037	-.0033	.0078	.0210	.0176	.0013	-.0008	-.0005	-.0002	-.0003	-.0002
25	-.0017	-.0032	-.0048	.0036	.0209	.0163	.0017	-.0008	-.0002	-.0002	-.0004	-.0002
30	0	-.0068	-.0029	.0015	.0117	.0160	.0020	-.0012	-.0005	-.0002	-.0004	-.0003
	$C_{n_{\delta_s}}$, per deg			$C_{l_{\delta_s}}$, per deg			C_{Y_p}, per rad			C_{n_p}, per rad		
-10	0.0007	0.0007	0.0005	0.0015	0.0023	0.0024	-0.02	-0.09	-0.49	-0.15	-0.11	0.38
-5	.0008	.0008	.0009	.0020	.0029	.0028	-.04	-.04	-.10	-.04	-.15	-.12
0	.0009	.0009	.0013	.0025	.0035	.0032	0	.05	.11	-.02	-.22	-.30
5	.0009	.0010	.0015	.0027	.0038	.0033	.07	.19	.10	-.20	-.28	-.25
10	.0009	.0011	.0015	.0026	.0038	.0032	.05	.25	.53	-.16	-.33	-.40
15	.0009	.0011	.0015	.0022	.0036	.0031	.24	.45	.80	-.20	-.45	-.52
20	.0008	.0011	.0014	.0017	.0035	.0029	.30	.80	1.20	-.22	-.50	-.57
25	.0008	.0010	.0013	.0011	.0037	.0028	.06	.89	1.25	-.15	-.40	-.59
30	.0007	.0010	.0012	.0008	.0038	.0028	.13	.75	1.03	-.14	-.22	-.15
	$C_{X_{\delta_t}}$, per deg			$C_{Z_{\delta_t}}$, per deg			$C_{m_{\delta_t}}$, per deg			$C_{Y_{\delta_r}}$, per deg		
-10	-0.0092	0.0072	-0.0049	-0.0242	-0.0160	-0.0102	-0.090	-0.084	-0.028	0.012	0.010	0.009
-5	-.0062	.0042	-.0019	-.0246	-.0204	-.0101	-.085	-.087	-.044	.012	.010	.009
0	-.0030	.0010	.0010	-.0250	-.0250	-.0100	-.080	-.090	-.060	.012	.010	.009
5	-.0002	-.0012	.0004	-.0201	-.0202	-.0050	-.065	-.097	-.076	.011	.010	.009
10	-.0036	-.0044	-.0070	-.0138	-.0211	-.0174	-.040	-.092	-.088	.010	.010	.009
15	-.0018	-.0071	-.0015	-.0088	-.0122	-.0252	-.013	-.078	-.098	.010	.010	.010
20	-.0006	-.0011	.0002	-.0042	-.0057	-.0180	.002	-.069	-.089	.009	.011	.010
25	-.0042	-.0051	-.0030	-.0053	-.0079	-.0124	.002	-.060	-.080	.006	.012	.012
30	-.0002	-.0152	.0339	-.0036	-.0312	-.0728	-.005	-.050	-.079	.002	.010	.012

TABLE II.- BASIC AERODYNAMIC INPUTS USED IN SIMULATION – Continued

α, deg	C_T=0	C_T=1.87	C_T=3.74	C_T=0	C_T=1.87	C_T=3.74	C_T=0	C_T=1.87	C_T=3.74	C_T=0	C_T=1.87	C_T=3.74
	$C_{n_{\delta_r}}$, per deg			$C_{l_{\delta_r}}$, per deg			C_{l_p}, per rad			C_{Y_r}, per rad		
-10	-0.0043	-0.0051	-0.0046	0.0020	0.0016	0.0019	-0.05	-1.13	-0.78	0.76	0.88	0.94
-5	-.0041	-.0047	-.0046	.0018	.0016	.0020	-.60	-.88	-.75	.76	.86	.92
0	-.0039	-.0043	-.0046	.0016	.0016	.0021	-.98	-.68	-.72	.77	.90	1.00
5	-.0038	-.0041	-.0046	.0016	.0017	.0022	-.68	-.50	-.68	.77	1.03	1.20
10	-.0036	-.0040	-.0046	.0016	.0017	.0022	-.40	-.50	-.63	.78	1.08	1.60
15	-.0034	-.0040	-.0046	.0011	.0017	.0022	-.37	-.50	-.55	.80	1.00	1.35
20	-.0024	-.0040	-.0046	.0003	.0016	.0020	-.32	-.33	-.42	.59	.70	1.24
25	-.0020	-.0041	-.0047	-.0003	.0010	.0017	-.26	-.17	-.33	.33	.32	.93
30	-.0002	-.0033	-.0042	.0006	.0008	.0014	-.26	-.08	-.25	-.08	1.70	2.55
	C_{Y_β}, per deg			C_{n_β}, per deg			C_{l_β}, per deg			$C_{X_{\delta_{sp}}}$, per deg		
-10	-0.020	-0.022	-0.050	0.0030	0.0035	0.0053	0.0012	0	0	0	-0.0060	-0.0044
-5	-.020	-.050	-.050	.0038	.0052	.0070	-.0006	-.0020	-.0020	-.0016	-.0043	-.0042
0	-.020	-.050	-.055	.0042	.0078	.0081	-.0024	-.0036	-.0031	-.0040	-.0010	-.0040
5	-.020	-.050	-.055	.0043	.0082	.0086	-.0034	-.0048	-.0044	-.0048	-.0018	-.0056
10	-.020	-.050	-.055	.0043	.0080	.0081	-.0023	-.0051	-.0053	-.0052	-.0016	-.0045
15	-.023	-.050	-.055	.0047	.0082	.0089	-.0028	-.0051	-.0061	-.0046	-.0012	-.0080
20	-.024	-.050	-.055	.0050	.0084	.0092	-.0029	-.0062	-.0066	-.0036	-.0046	-.0070
25	-.020	-.050	-.055	.0021	.0083	.0088	-.0070	-.0067	-.0072	.0001	-.0025	-.0085
30	-.024	-.020	-.055	.0018	-.0040	.0082	-.0050	-.0070	-.0090	.0012	-.0082	-.0024
	$C_{Z_{\delta_{sp}}}$, per deg			$C_{m_{\delta_{sp}}}$, per deg			C_{n_r}, per rad			C_{l_r}, per rad		
-10	0.0260	0.0430	0.0300	-0.006	0	0.008	-0.45	-0.33	-0.37	0.32	0.57	0.55
-5	.0272	.0425	.0325	-.004	0	.005	-.35	-.38	-.42	.48	.70	.77
0	.0290	.0420	.0380	-.002	0	.002	-.30	-.42	-.45	.67	.80	.86
5	.0317	.0440	.0417	0	0	.001	-.33	-.41	-.45	.77	.85	.85
10	.0296	.0434	.0429	.001	0	.001	-.34	-.42	-.54	.83	.80	.80
15	.0247	.0432	.0414	.004	.001	.002	-.38	-.42	-.52	.88	.82	.83
20	.0157	.0420	.0387	.005	.001	.002	-.35	-.40	-.52	.73	.90	.90
25	.0045	.0408	.0347	.004	.001	.003	-.30	-.34	-.47	.83	1.10	.93
30	.0019	-.0022	.0321	.004	.001	.003	-.20	-.42	-.70	.62	-.20	-.50

α, deg	C_T=0	C_T=0.70	C_T=1.40	C_T=2.10	C_T=2.81	C_T=0	C_T=0.70	C_T=1.40	C_T=2.10	C_T=2.81	C_T=0	C_T=0.70	C_T=1.40	C_T=2.10	C_T=2.81
	$C_{Y_{\delta_a}}$, per deg					$C_{n_{\delta_a}}$, per deg					$C_{l_{\delta_a}}$, per deg				
-10	-0.0016	-0.0010	-0.0004	0.0002	0.0008	-0.0014	-0.0028	-0.0040	-0.0052	-0.0064	0.0082	0.0083	0.0084	0.0085	0.0086
-5	-.0012	-.0007	-.0002	.0003	.0008	-.0001	-.0017	-.0032	-.0047	-.0062	.0048	.0058	.0068	.0078	.0088
0	-.0008	-.0004	0	.0004	.0008	.0012	-.0006	-.0024	-.0042	-.0060	.0014	.0033	.0052	.0071	.0090
5	-.0004	-.0002	0	.0002	.0004	-.0010	-.0022	-.0034	-.0046	-.0058	.0014	.0033	.0052	.0071	.0090
10	-.0006	-.0004	-.0002	0	.0002	-.0010	-.0022	-.0034	-.0046	-.0058	.0010	.0030	.0050	.0070	.0090
15	-.0008	-.0006	-.0004	-.0002	.0001	.0004	-.0011	-.0026	-.0041	-.0056	.0027	.0044	.0061	.0078	.0096
20	-.0022	-.0018	-.0014	-.0010	-.0005	.0045	.0026	.0007	-.0012	-.0032	.0207	.0197	.0187	.0177	.0168
25	-.0036	-.0024	-.0012	0	-.0012	.0036	.0024	.0010	-.0002	-.0014	-.0010	.0050	.0110	.0170	.0240
30	-.0007	-.0006	-.0005	-.0004	-.0003	.0024	.0008	-.0008	-.0024	-.0040	-.0076	-.0012	.0052	.0116	.0180

TABLE II.- BASIC AERODYNAMIC INPUTS USED IN SIMULATION – Concluded

α, deg	$\delta_{f3}=35^{o}$	$\delta_{f3}=45^{o}$	$\delta_{f3}=60^{o}$	$\delta_{f3}=70^{o}$	$\delta_{f3}=35^{o}$	$\delta_{f3}=45^{o}$	$\delta_{f3}=60^{o}$	$\delta_{f3}=70^{o}$
	C_X for $C_T = 0$				C_X for $C_T = 0.94$			
-10	-0.126	-0.200	-0.229	-0.246	0.397	0.140	-0.248	-0.502
-5	-.224	-.285	-.366	-.330	.319	.033	-.398	-.518
0	-.210	-.258	-.340	-.300	.320	.090	-.300	-.450
5	-.110	-.167	-.248	-.218	.403	.189	-.184	-.339
10	.040	-.031	-.115	-.100	.555	.349	-.011	-.180
15	.181	.099	.018	.035	.725	.511	.181	.011
20	.271	.186	.091	.137	.882	.679	.358	.201
25	.314	.222	.078	.159	1.005	.812	.471	.384
30	.339	.226	.111	.168	1.101	.867	.452	.549
	C_X for $C_T = 1.87$				C_X for $C_T = 3.74$			
-10	0.919	0.477	-0.233	-0.768	2.124	1.401	0.319	-0.561
-5	.852	.408	-.231	-.716	2.054	1.300	.285	-.435
0	.850	.448	-.250	-.600	2.040	1.298	.300	-.350
5	.916	.551	-.119	-.470	2.117	1.399	.432	-.251
10	1.059	.723	.096	-.262	2.262	1.559	.594	-.061
15	1.262	.922	.344	-.011	2.459	1.811	.932	.207
20	1.496	1.173	.633	.261	2.678	2.062	1.162	.509
25	1.707	1.396	.863	.614	2.896	2.346	1.536	.811
30	1.868	1.500	.798	.921	3.121	2.577	1.765	1.212
	C_Z for $C_T = 0$				C_Z for $C_T = 0.94$			
-10	0.378	0.085	-0.055	0.043	-0.395	-0.776	-1.581	-1.577
-5	-.381	-.667	-.741	-.673	-1.173	-1.629	-2.254	-2.364
0	-1.250	-1.440	-1.400	-1.410	-2.020	-2.490	-2.950	-3.130
5	-1.957	-2.173	-2.089	-2.097	-2.788	-3.256	-3.630	-3.804
10	-2.471	-2.645	-2.519	-2.485	-3.375	-3.807	-4.145	-4.276
15	-2.840	-2.844	-2.770	-2.797	-3.864	-4.180	-4.538	-4.677
20	-2.966	-2.912	-2.851	-2.802	-4.149	-4.414	-4.786	-4.908
25	-2.921	-2.886	-2.700	-2.707	-4.286	-4.553	-4.867	-4.940
30	-2.807	-2.791	-2.592	-2.651	-4.307	-4.373	-4.104	-4.591
	C_Z for $C_T = 1.87$				C_Z for $C_T = 3.74$			
-10	-1.178	-1.628	-3.107	-3.205	-1.948	-2.928	-4.524	-4.622
-5	-1.962	-2.595	-3.795	-4.053	-2.790	-3.818	-5.345	-5.543
0	-2.800	-3.540	-4.500	-4.850	-3.600	-4.720	-6.130	-6.500
5	-3.584	-4.328	-5.180	-5.522	-4.462	-5.540	-6.889	-7.230
10	-4.281	-4.980	-5.781	-6.057	-5.227	-6.264	-7.572	-7.830
15	-4.901	-5.511	-6.305	-6.567	-5.894	-6.876	-8.116	-8.423
20	-5.340	-5.916	-6.708	-7.003	-6.422	-7.391	-8.602	-8.913
25	-5.648	-6.223	-7.035	-7.162	-6.848	-7.799	-8.971	-9.309
30	-5.815	-5.935	-5.602	-6.535	-7.205	-8.085	-9.258	-9.519

TABLE III.- SIMULATOR CONTROL CHARACTERISTICS

Control	Maximum travel in –			Breakout force		Force gradient	
	deg	cm	in.	N	lbf	N/cm	lbf/in.
Column:							
Forward	9.9	13.97	5.50	13.3	3.0	14.0	8.0
Aft	20.5	25.25	9.94				
Wheel	±130.0	±37.34	±14.70	11.1	2.5	5.3	3.0
Pedal		10.80	4.25	31.1	7.0	28.9	16.5

TABLE IV.- PILOT RATING SYSTEM

CONTROLLABLE Capable of being controlled or managed in context of mission, with available pilot attention.	ACCEPTABLE May have deficiencies which warrant improvement, but adequate for mission. Pilot compensation, if required to achieve acceptable performance, is feasible.	SATISFACTORY Meets all requirements and expectations; good enough without improvement. Clearly adequate for mission.	Excellent, highly desirable.	1
			Good, pleasant, well behaved.	2
			Fair. Some mildly unpleasant characteristics. Good enough for mission without improvement.	3
		UNSATISFACTORY Reluctantly acceptable. Deficiencies which warrant improvement. Performance adequate for mission with feasible pilot compensation.	Some minor but annoying deficiencies. Improvement is requested. Effect on performance is easily compensated for by pilot.	4
			Moderately objectionable deficiencies. Improvement is needed. Reasonable performance requires considerable pilot compensation.	5
			Very objectionable deficiencies. Major improvements are needed. Requires best available pilot compensation to achieve acceptable performance.	6
	UNACCEPTABLE Deficiencies which require improvement. Inadequate performance for mission even with maximum feasible pilot compensation.		Major deficiencies which require improvement for acceptance. Controllable. Performance inadequate for mission, or pilot compensation required for minimum acceptable performance in mission is too high.	7
			Controllable with difficulty. Requires substantial pilot skill and attention to retain control and continue mission.	8
			Marginally controllable in mission. Requires maximum available pilot skill and attention to retain control.	9
UNCONTROLLABLE Control will be lost during some portion of mission.			Uncontrollable in mission.	10

TABLE V.- APPROXIMATE TIME REQUIRED TO ATTAIN AN ALTITUDE OF 152 m (500 ft), STARTING FROM h = 1219 m (4000 ft), WHEN MAINTAINING A GLIDE SLOPE OF 7.5°

[At constant speed {V = 75 knots, total time = 212 sec; V = 140 knots, total time = 113 sec}]

Piloting technique	Commanded deceleration rate, $\dot{V}$		Longitudinal deceleration, $\dot{V}$, g units		Time prior to initiation of deceleration, sec	Time of deceleration, sec	Total time, sec
	m/sec^2	ft/sec^2	Commanded	Maximum attained			
1 (PR = 3.5)	0.30	1	0.03	0.03	23	117	140
1 (PR = 4.5)	.61	[a]2	.06	[a].14	65	65	[a]130
1 (PR = 7)	.91	3	.09	.18	81	40	121
2 (PR = 1.5)	0.30	1	0.03	0.03	23	118	141
2 (PR = 1.5)	.61	2	.06	.06	65	65	130
2 (PR = 1.5)	1.22	[a]4	.12	[a].12	88	33	[a]121
2 (PR = 1.5)	2.44	8	.25	.26	94	27	121
2 (PR = 1.5)	3.05	10	.31	.30	94	27	121
3 (PR = 2)	0.30	1	0.03	0.03	23	118	141
3 (PR = 2)	.61	2	.06	.06	65	65	130
3 (PR = 2)	1.22	[a]4	.12	[a].13	88	34	[a]122
3 (PR = 2)	2.44	8	.25	.24	94	27	121
3 (PR = 2)	3.05	10	.31	.25	94	27	121
4 (PR = 3)	0.30	1	0.03	0.03	23	118	141
4 (PR = 3)	.61	[a]2	.06	[a].08	65	63	[a]128

[a]Maximum suggested deceleration rate.

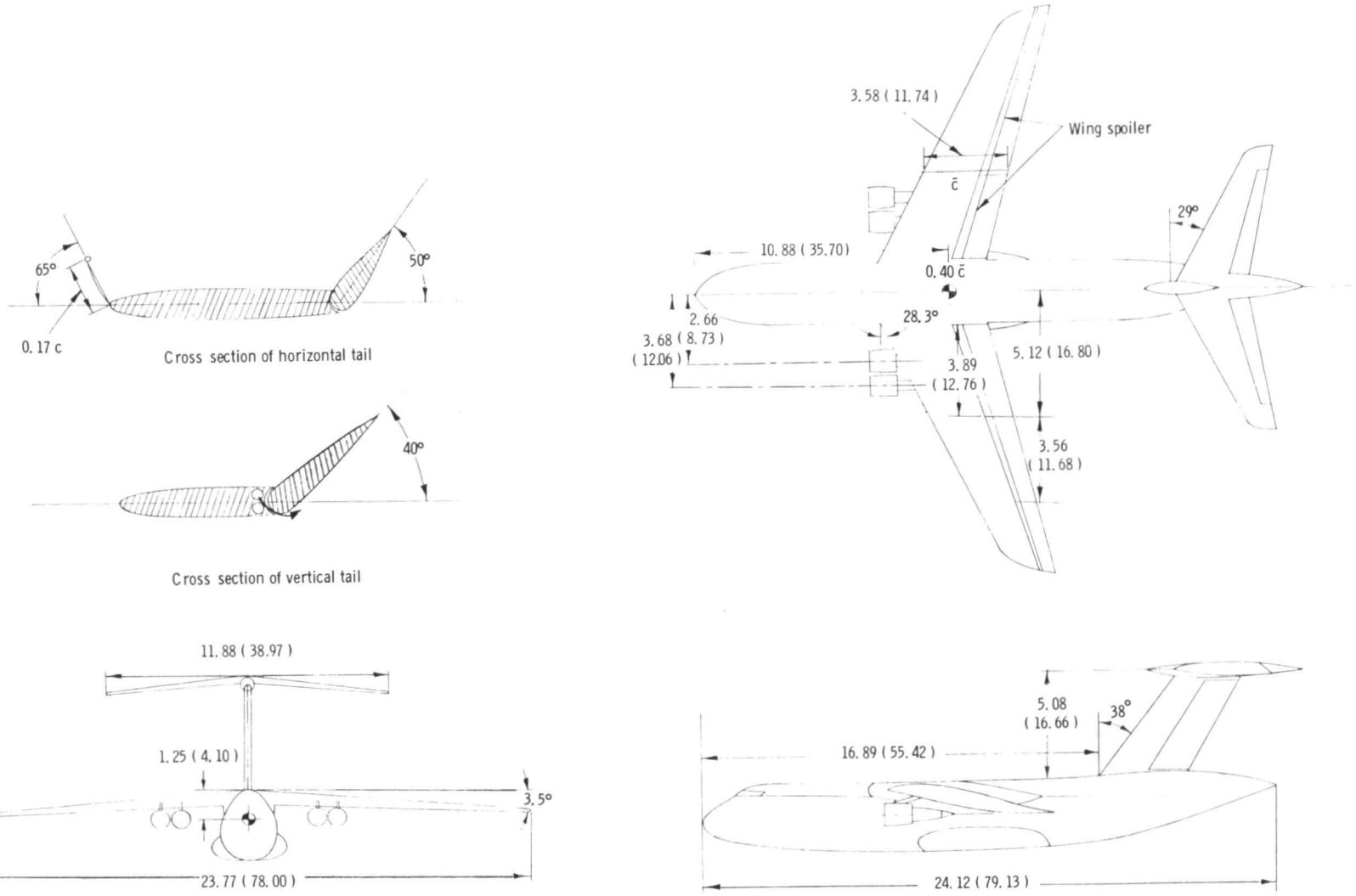

(a) Three-view drawing of simulated airplane. All linear dimensions are in meters (feet).

Figure 1.- Drawing of simulated airplane and flap assembly.

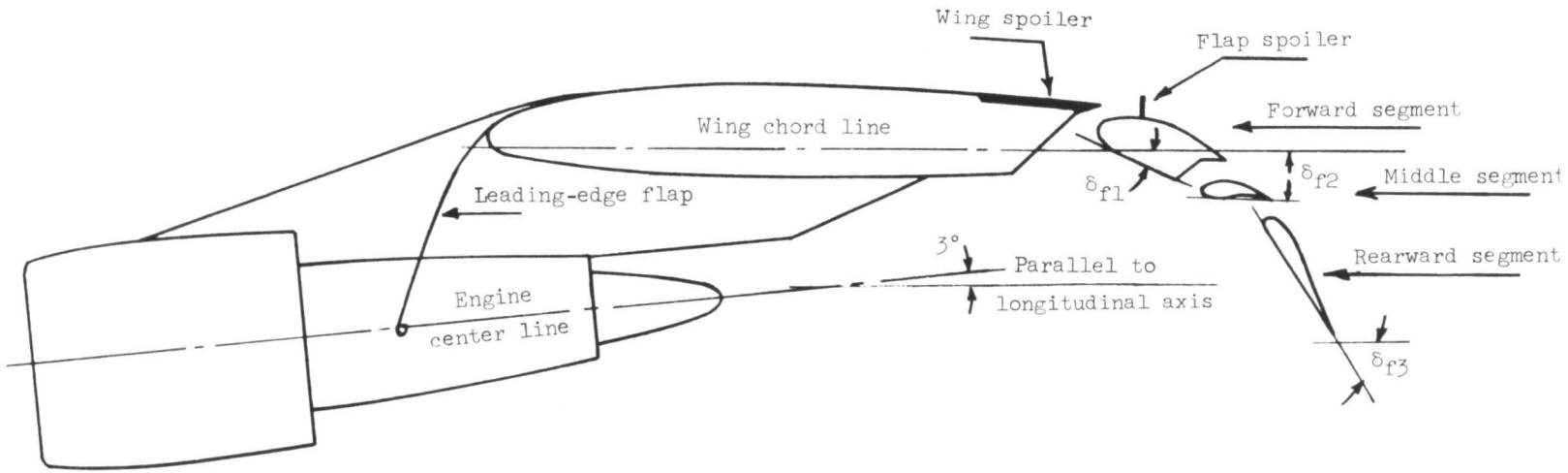

(b) Flap assembly and engine-pylon detail; $\delta_{f1}/\delta_{f2}/\delta_{f3} = 25/10/60$.

Figure 1.- Concluded.

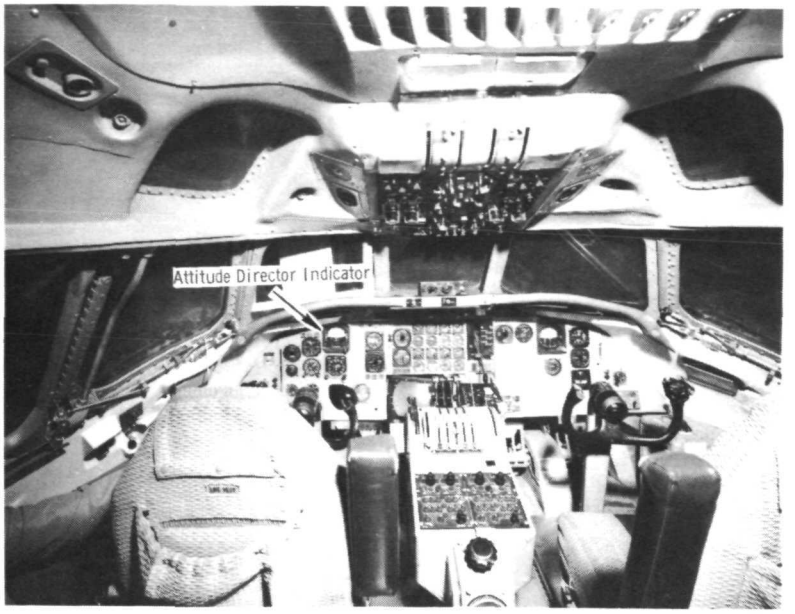

L-72-3813.2

(a) Simulator cockpit.

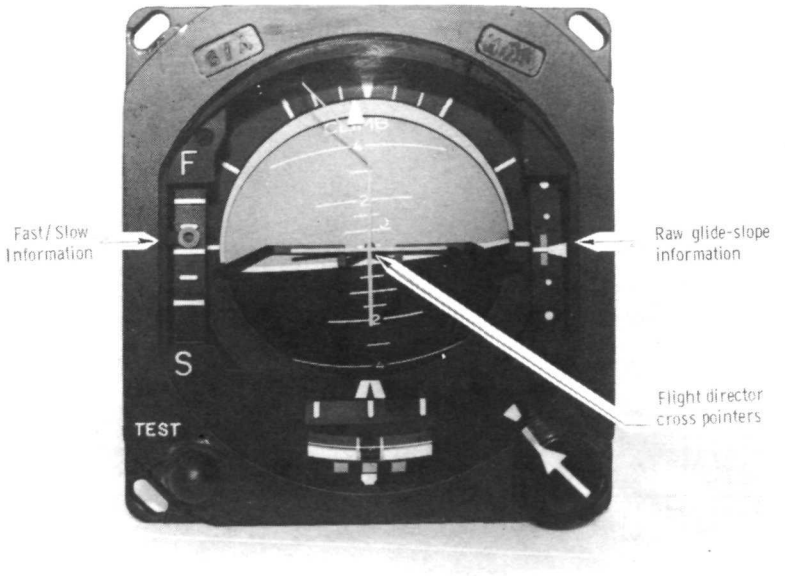

L-73-4451.1

(b) Attitude director indicator (ADI).

Figure 2.- Simulator cockpit and instrument display.

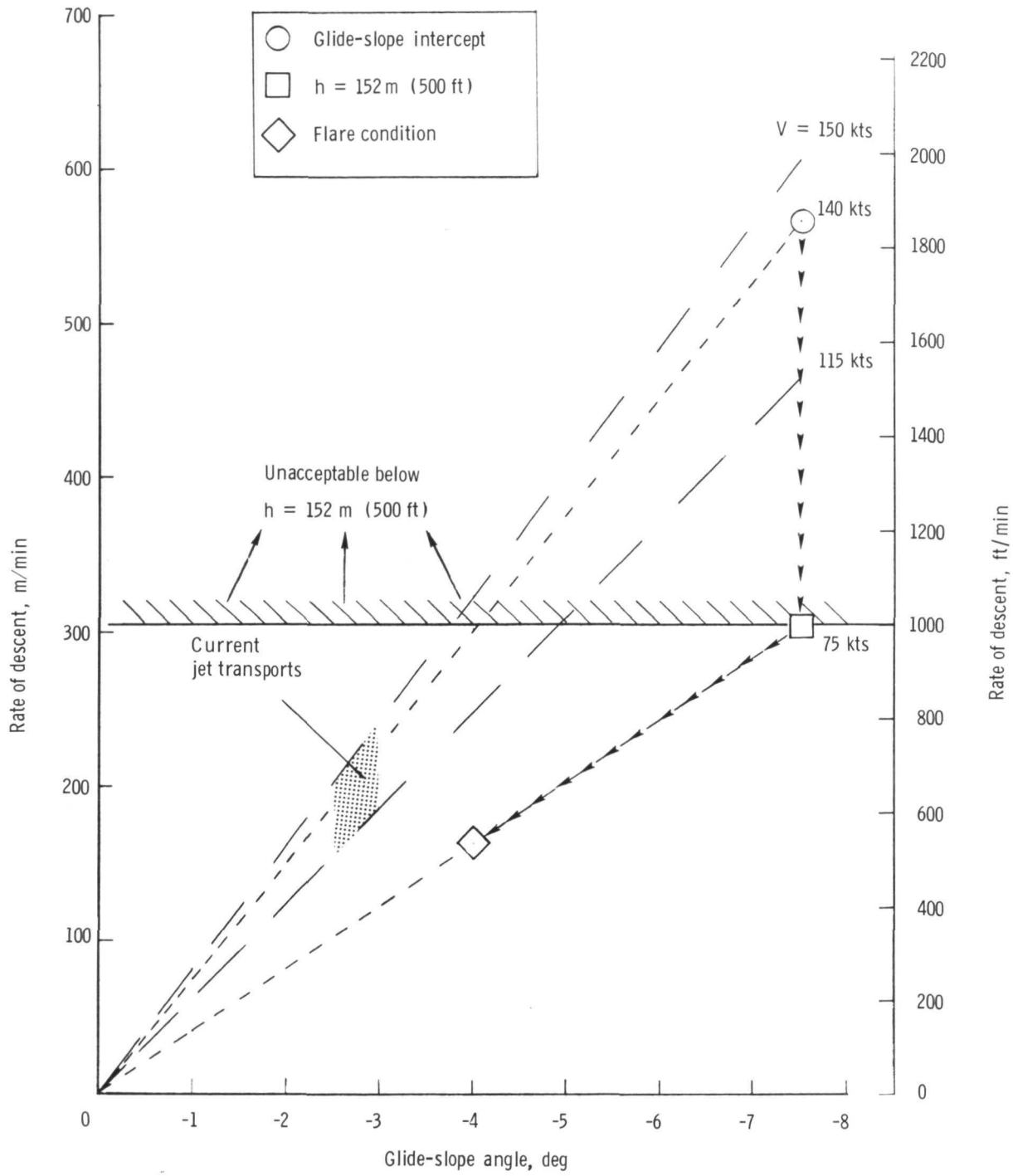

Figure 3.- Variation of rate of descent with glide-slope angle and airspeed for approaches used in this simulation.

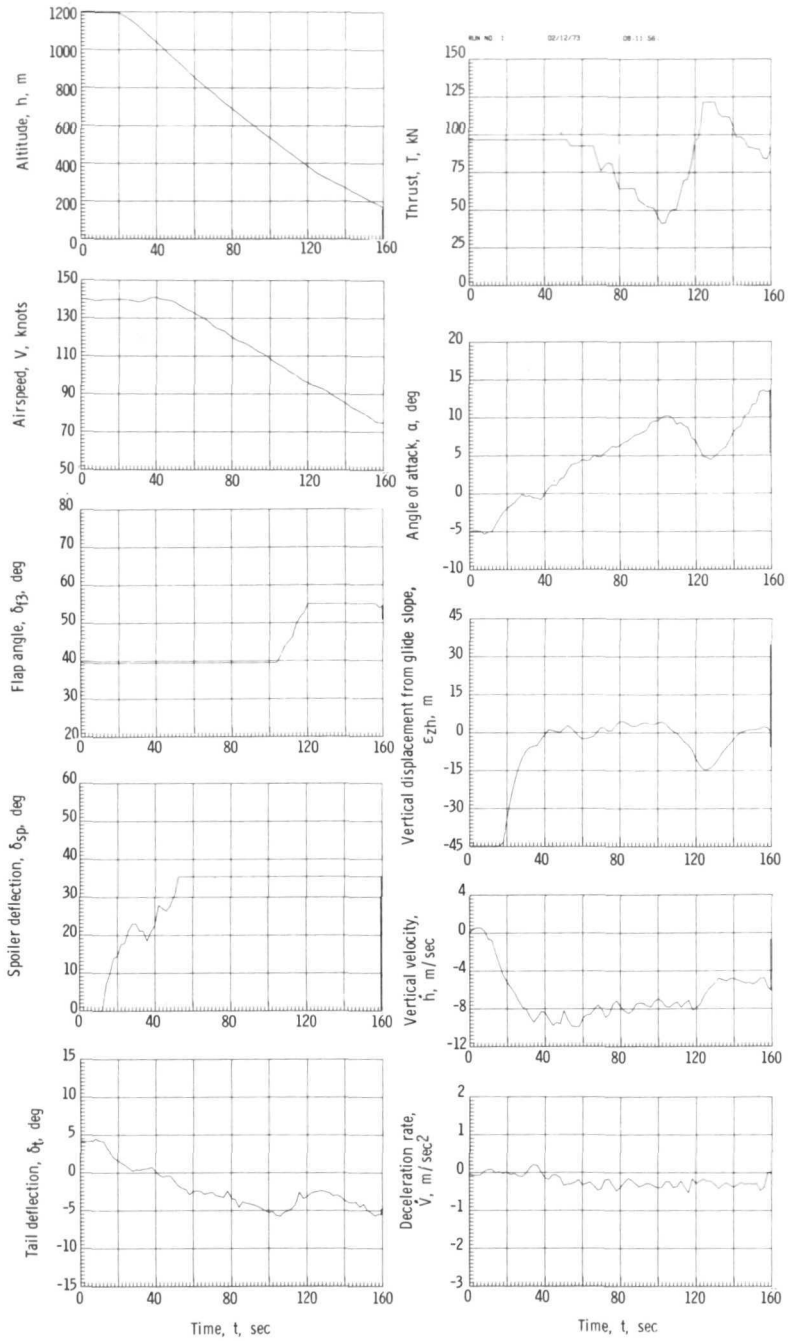

(a) Commanded deceleration rate of 0.30 m/sec^2 (1 ft/sec^2).

Figure 4.- Typical time histories of motions experienced during decelerating approaches using technique 1.

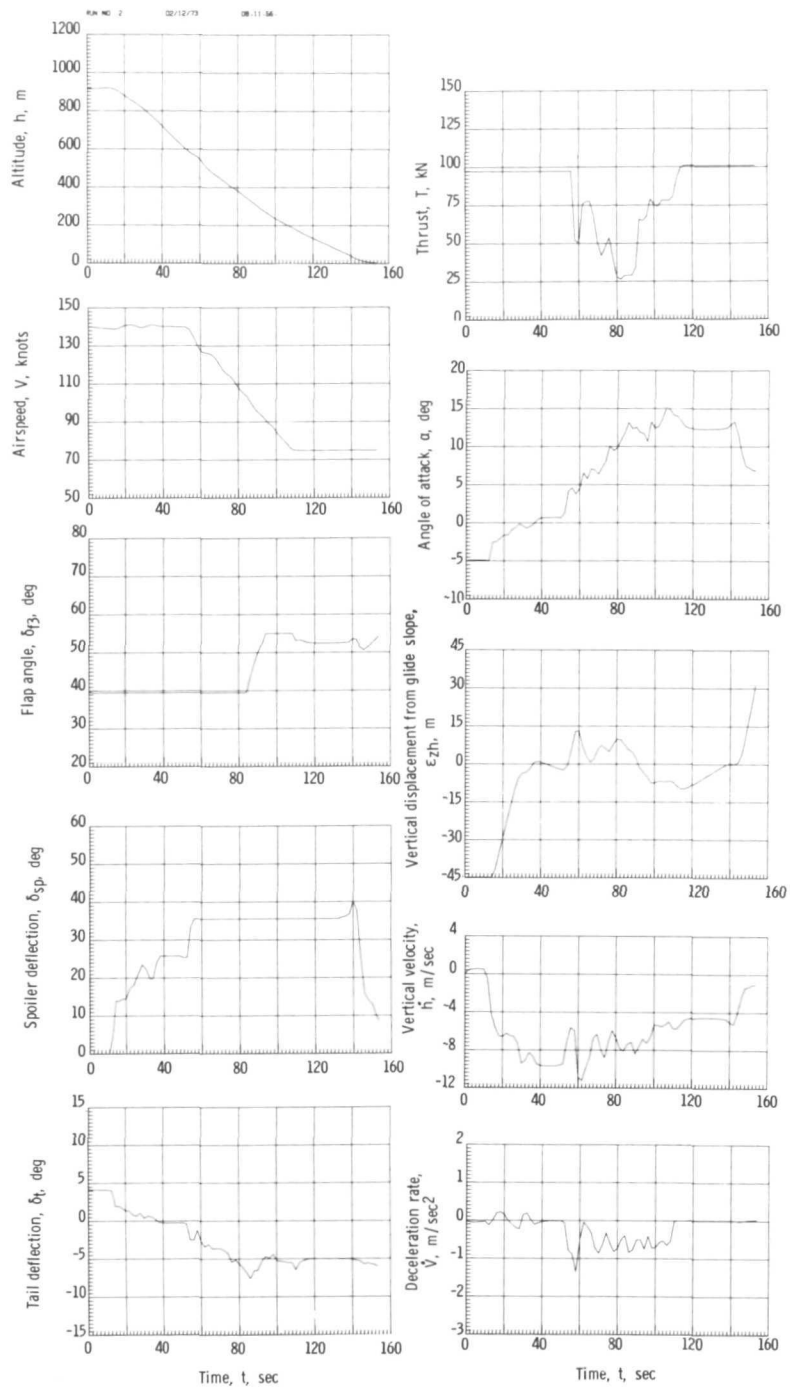

(b) Commanded deceleration rate of 0.61 m/sec^2 (2 ft/sec^2).

Figure 4.- Continued.

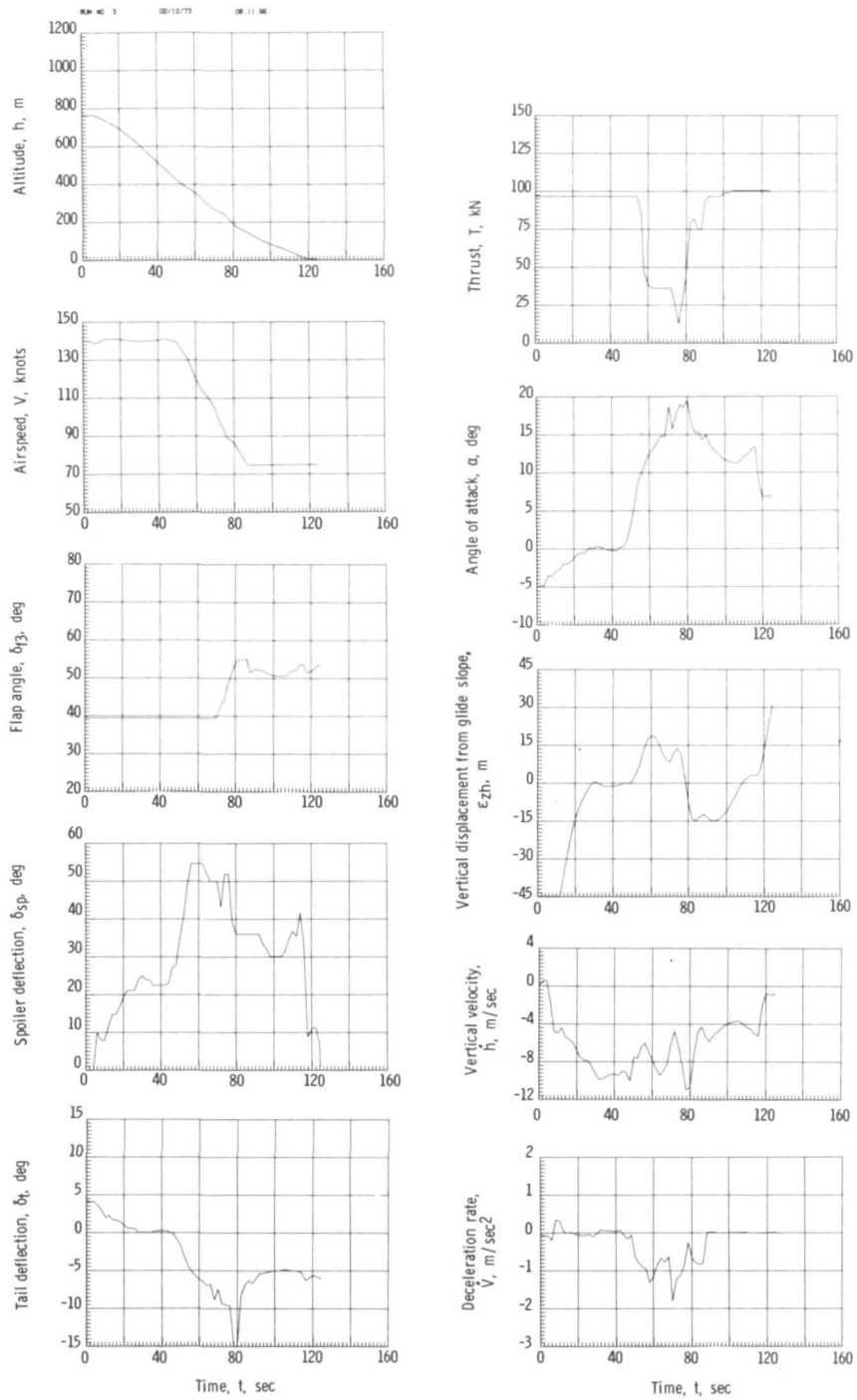

(c) Commanded deceleration rate of 0.91 m/sec^2 (3 ft/sec^2).

Figure 4.- Concluded.

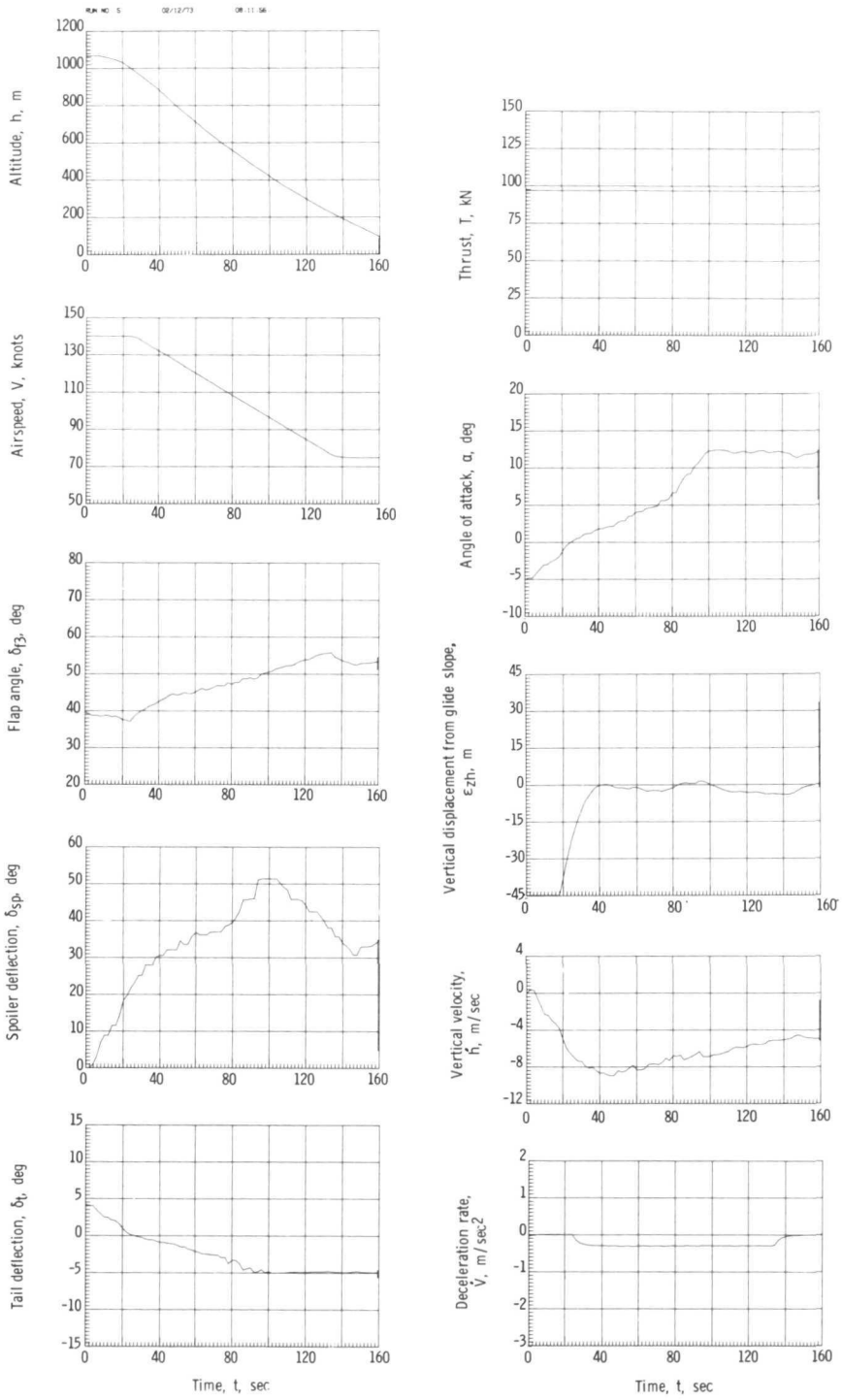

(a) Commanded deceleration rate of 0.30 m/sec^2 (1 ft/sec^2).

Figure 5.- Typical time histories of motions experienced during decelerating approaches using technique 2.

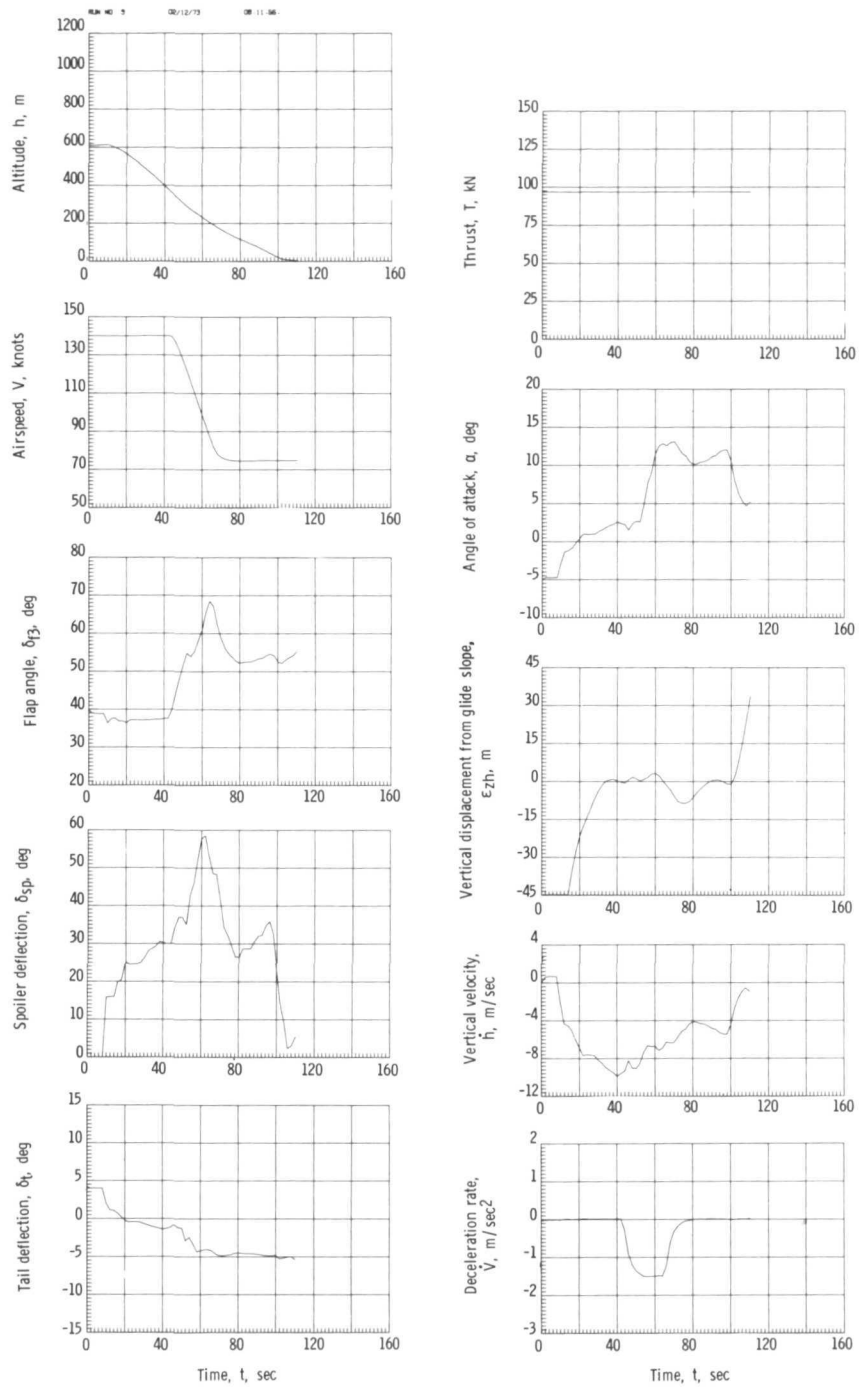

(b) Commanded deceleration rate of 1.52 m/sec^2 (5 ft/sec^2).

Figure 5.- Continued.

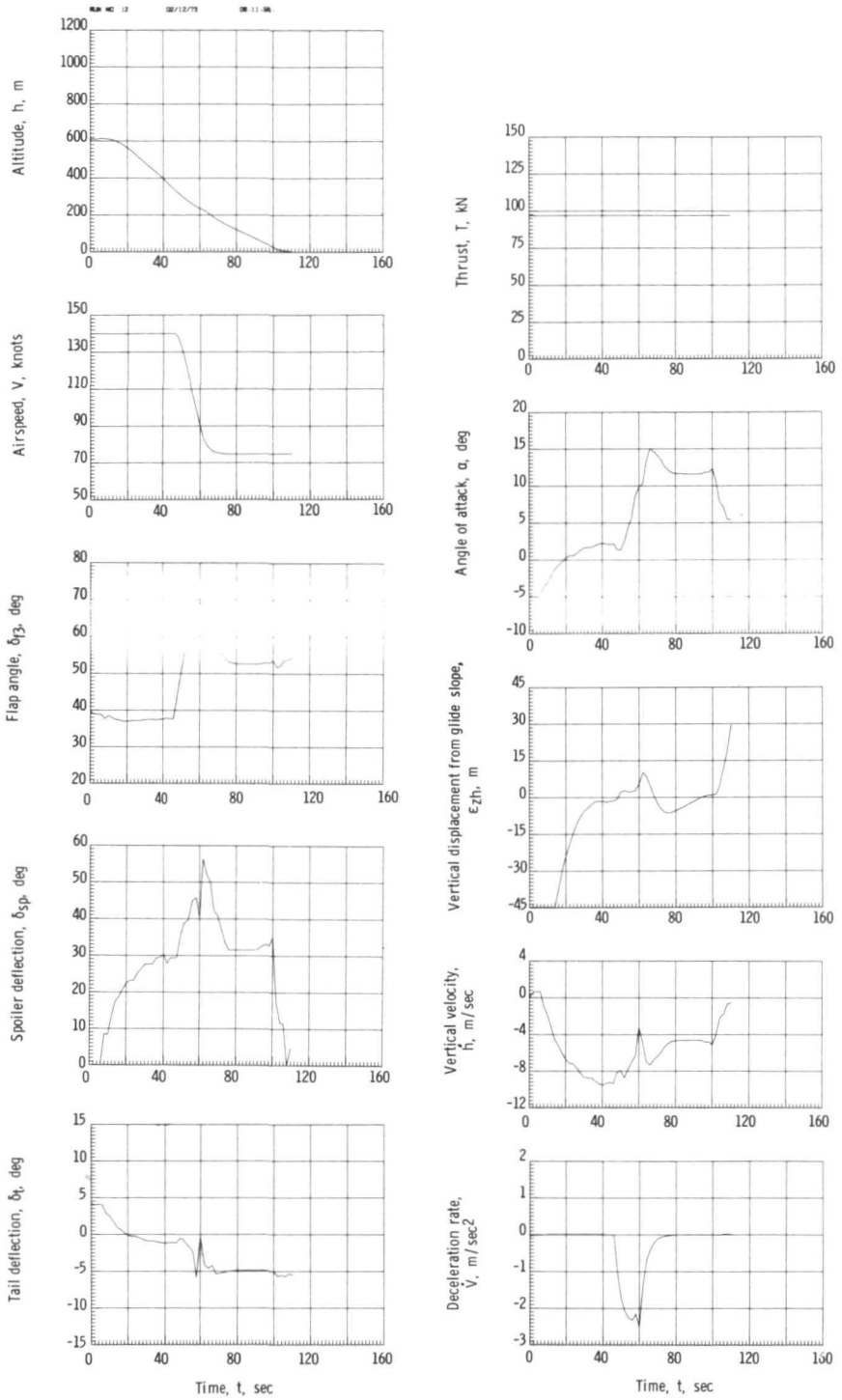

(c) Commanded deceleration rate of 2.44 m/sec^2 (8 ft/sec^2).

Figure 5.- Continued.

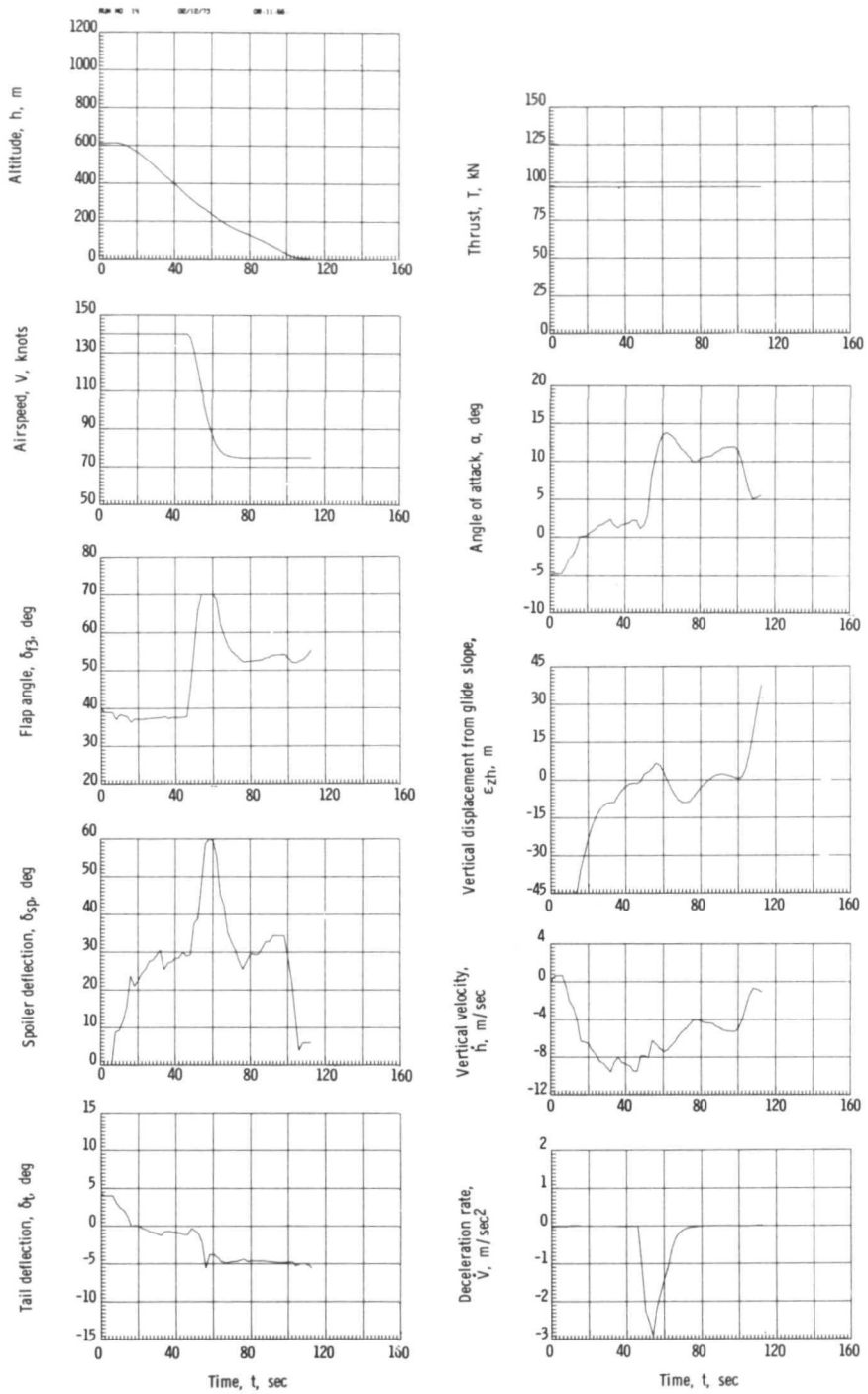

(d) Commanded deceleration rate of 3.05 m/sec^2 (10 ft/sec^2).

Figure 5.- Concluded.

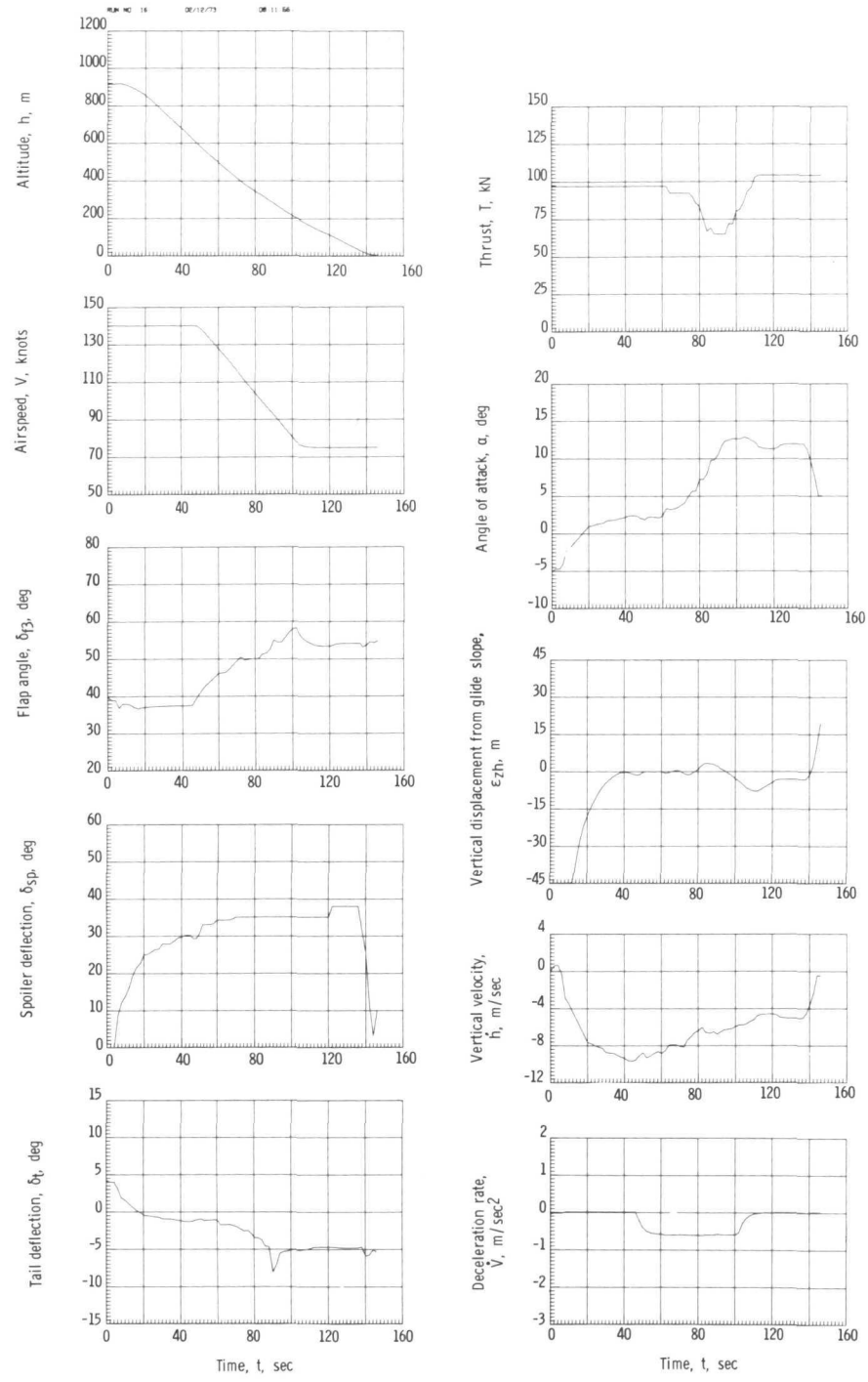

(a) Commanded deceleration rate of 0.61 m/sec^2 (2 ft/sec^2).

Figure 6.- Typical time histories of motions experienced during decelerating approaches using technique 3.

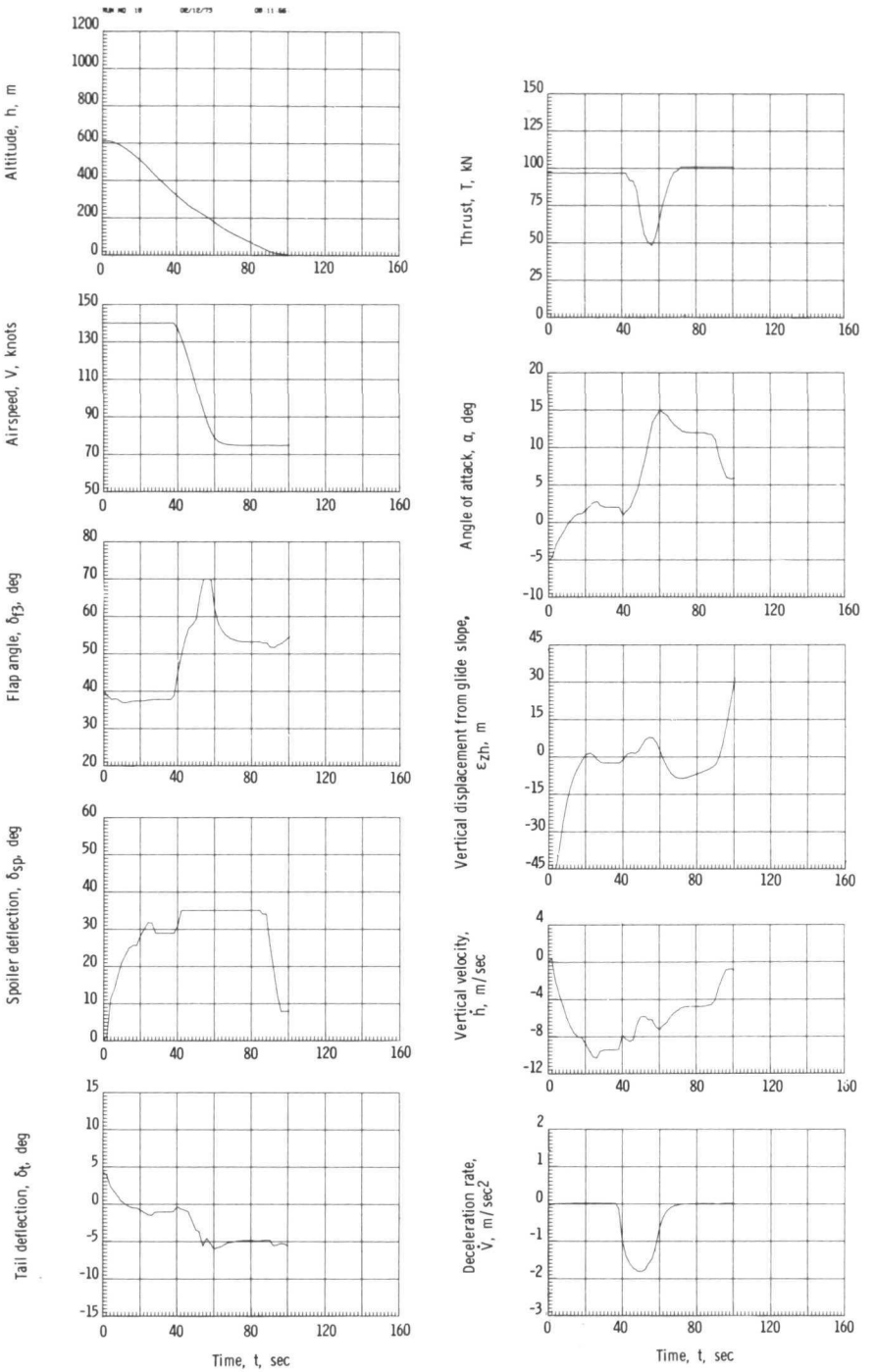

(b) Commanded deceleration rate of 1.83 m/sec^2 (6 ft/sec^2).

Figure 6.- Continued.

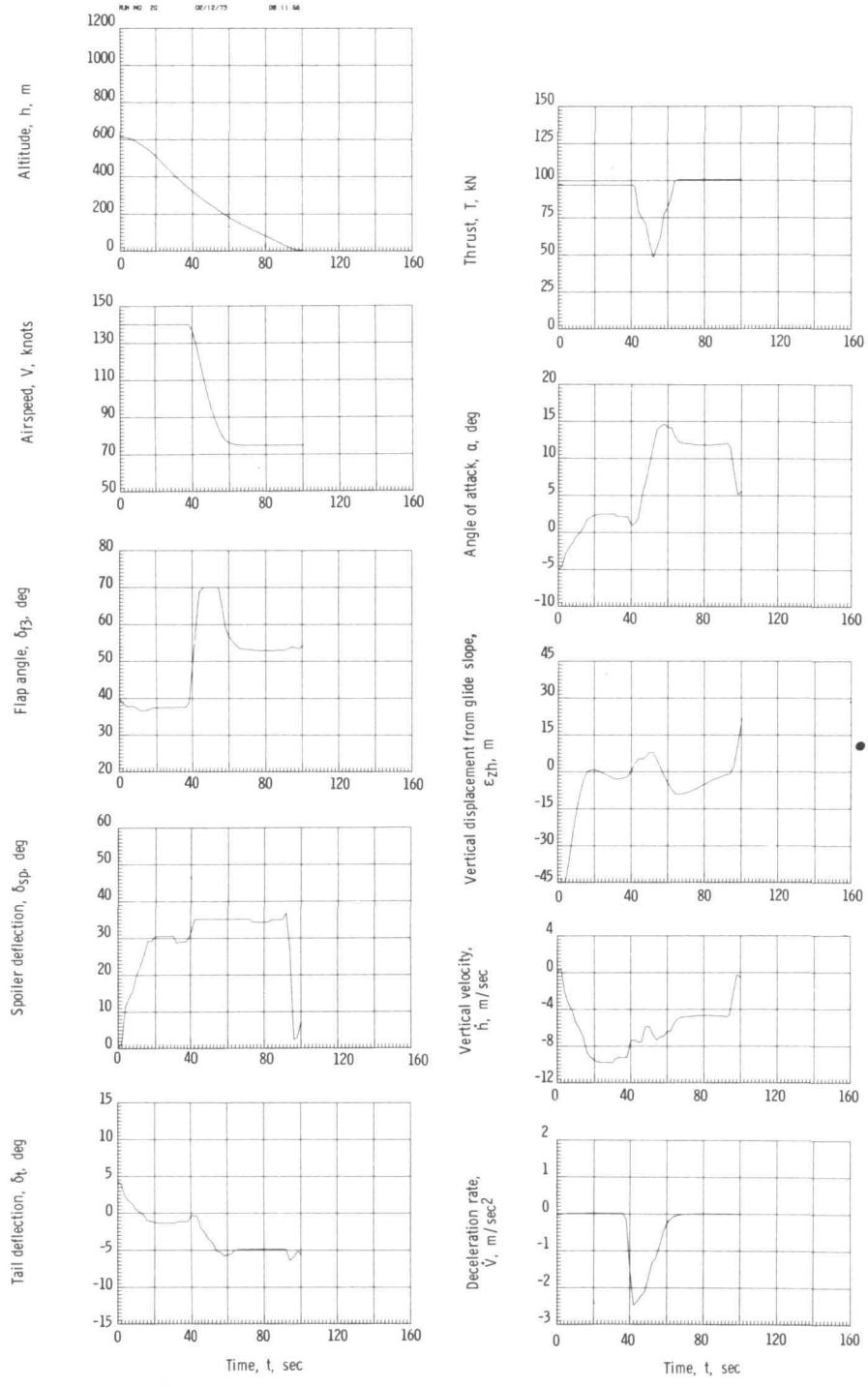

(c) Commanded deceleration rate of 3.05 m/sec^2 (10 ft/sec^2).

Figure 6.- Concluded.

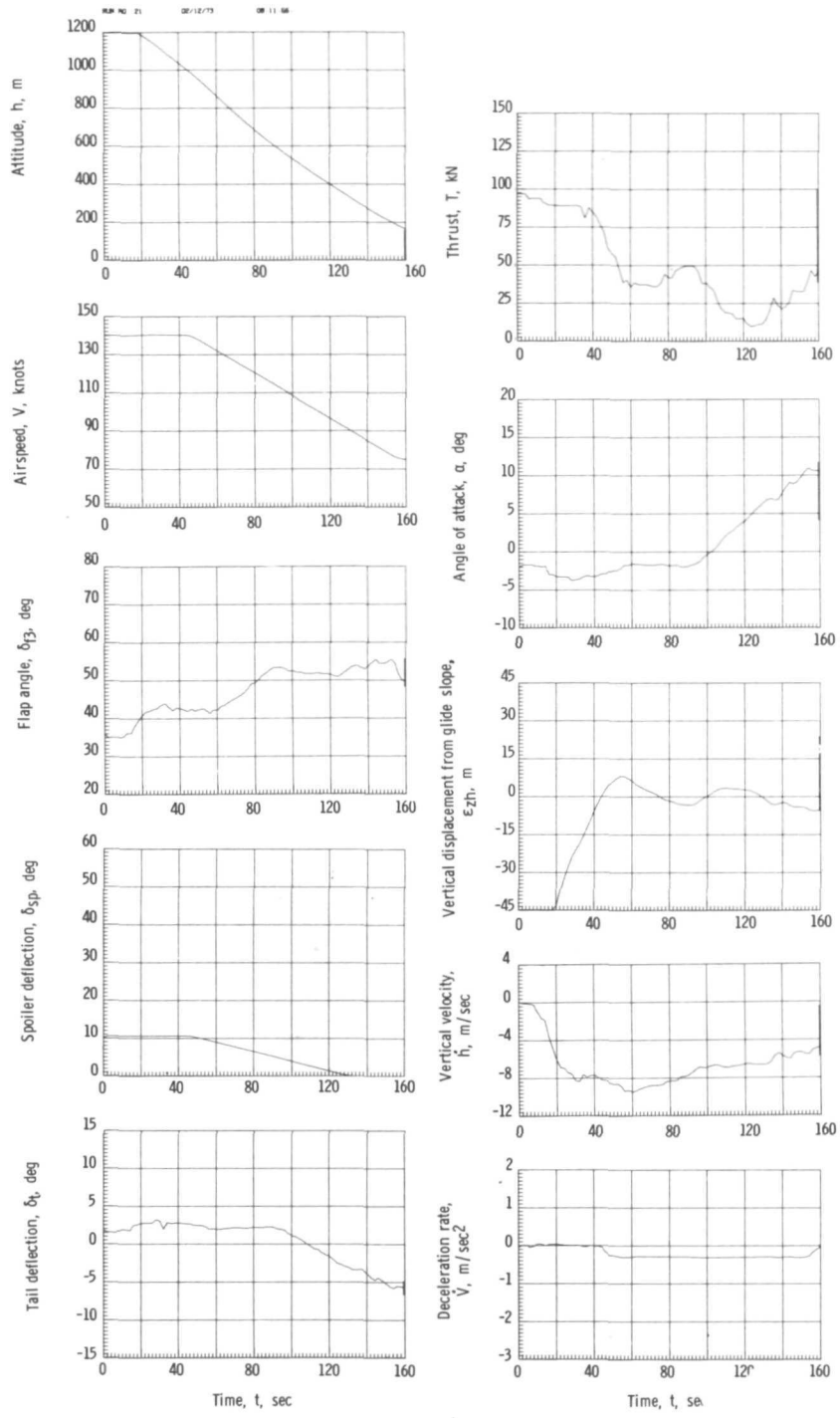

(a) Commanded deceleration rate of 0.30 m/sec^2 (1 ft/sec^2).

Figure 7.- Typical time histories of motions experienced during decelerating approaches using technique 4.

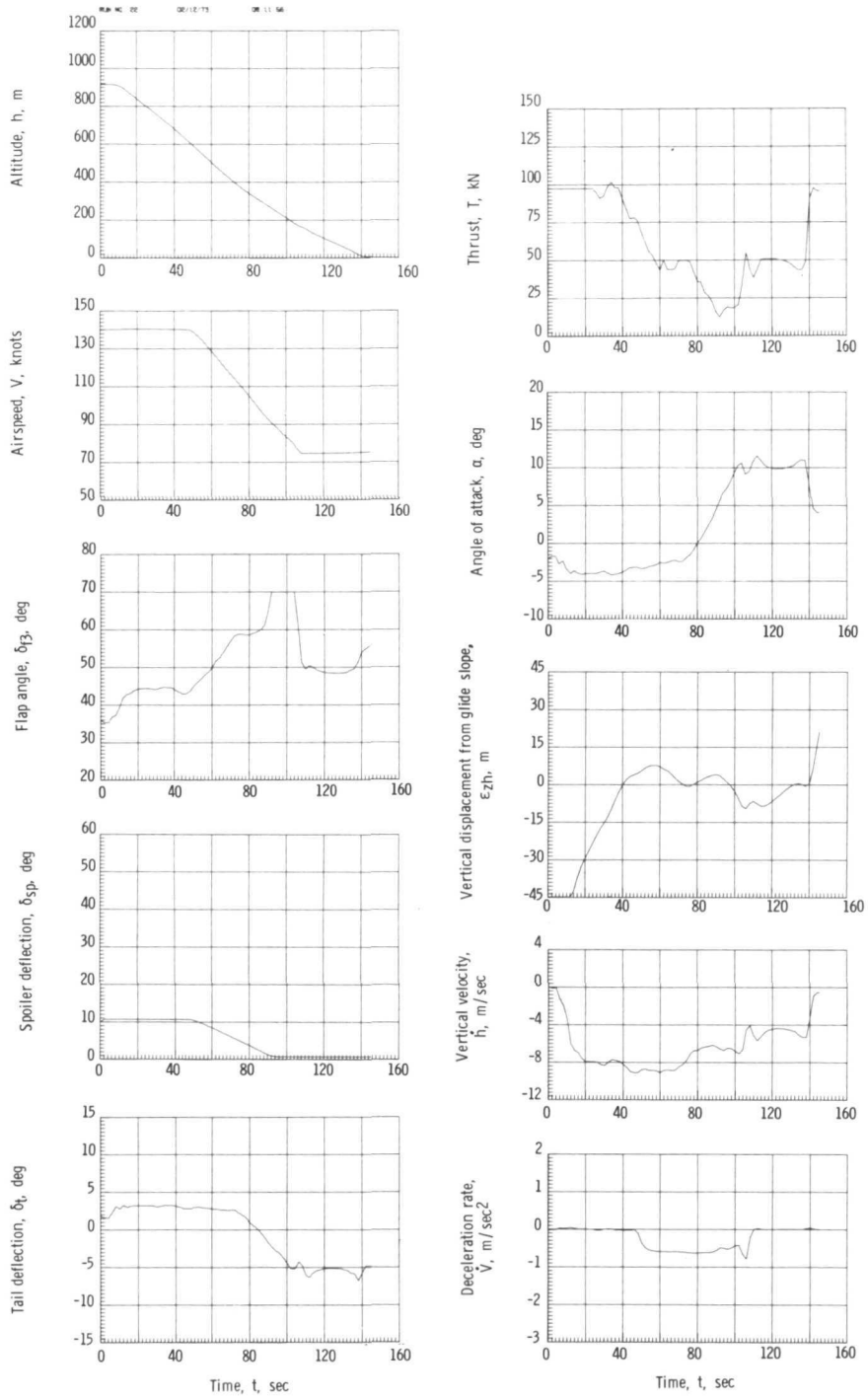

(b) Commanded deceleration rate of 0.61 m/sec^2 (2 ft/sec^2).

Figure 7.- Continued.

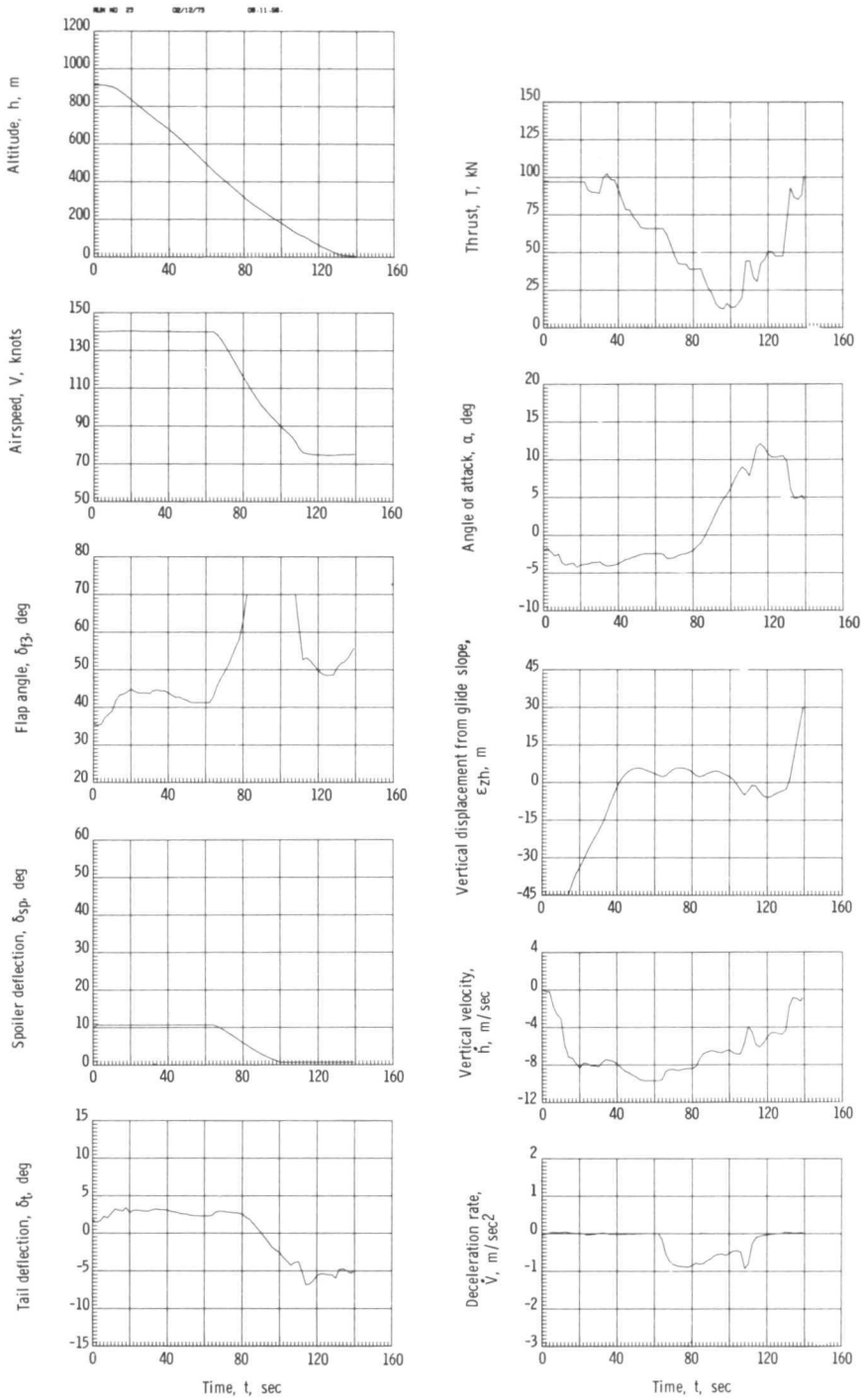

(c) Commanded deceleration rate of 0.91 m/sec^2 (3 ft/sec^2).

Figure 7.- Continued.

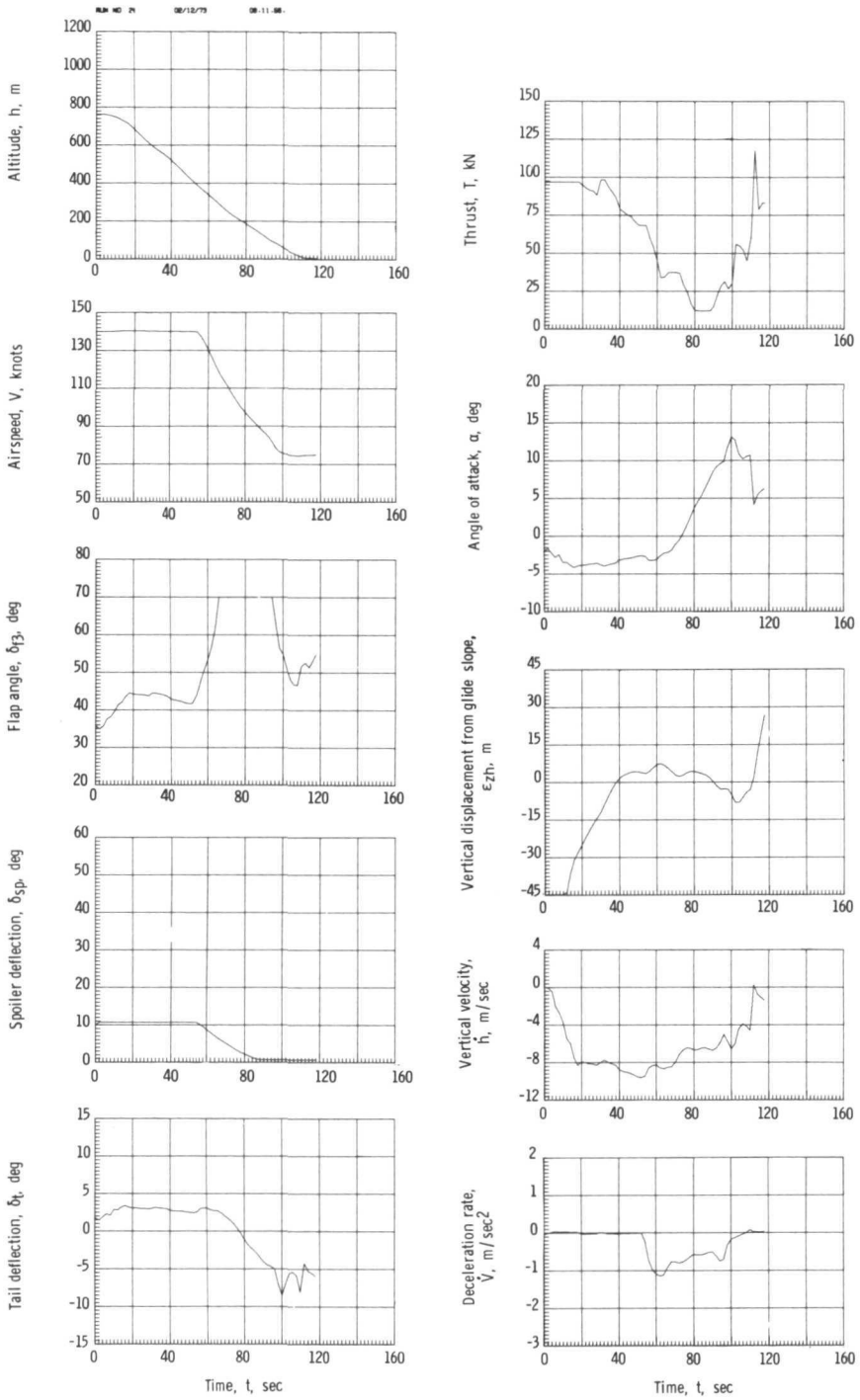

(d) Commanded deceleration rate of 1.22 m/sec^2 (4 ft/sec^2).

Figure 7.- Concluded.

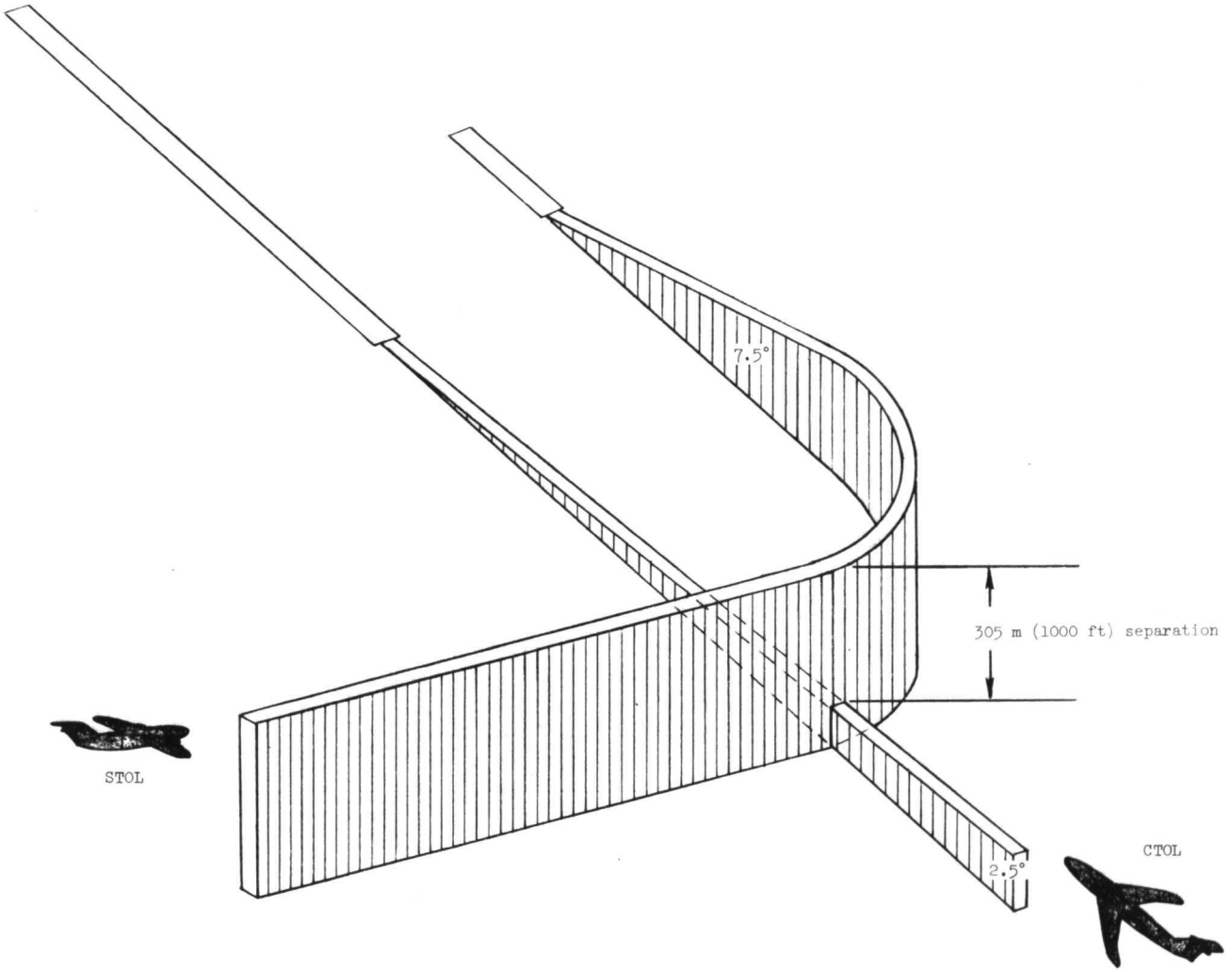

Figure 8.- Possible curved, steep gradient approach profile for future STOL jet transports.

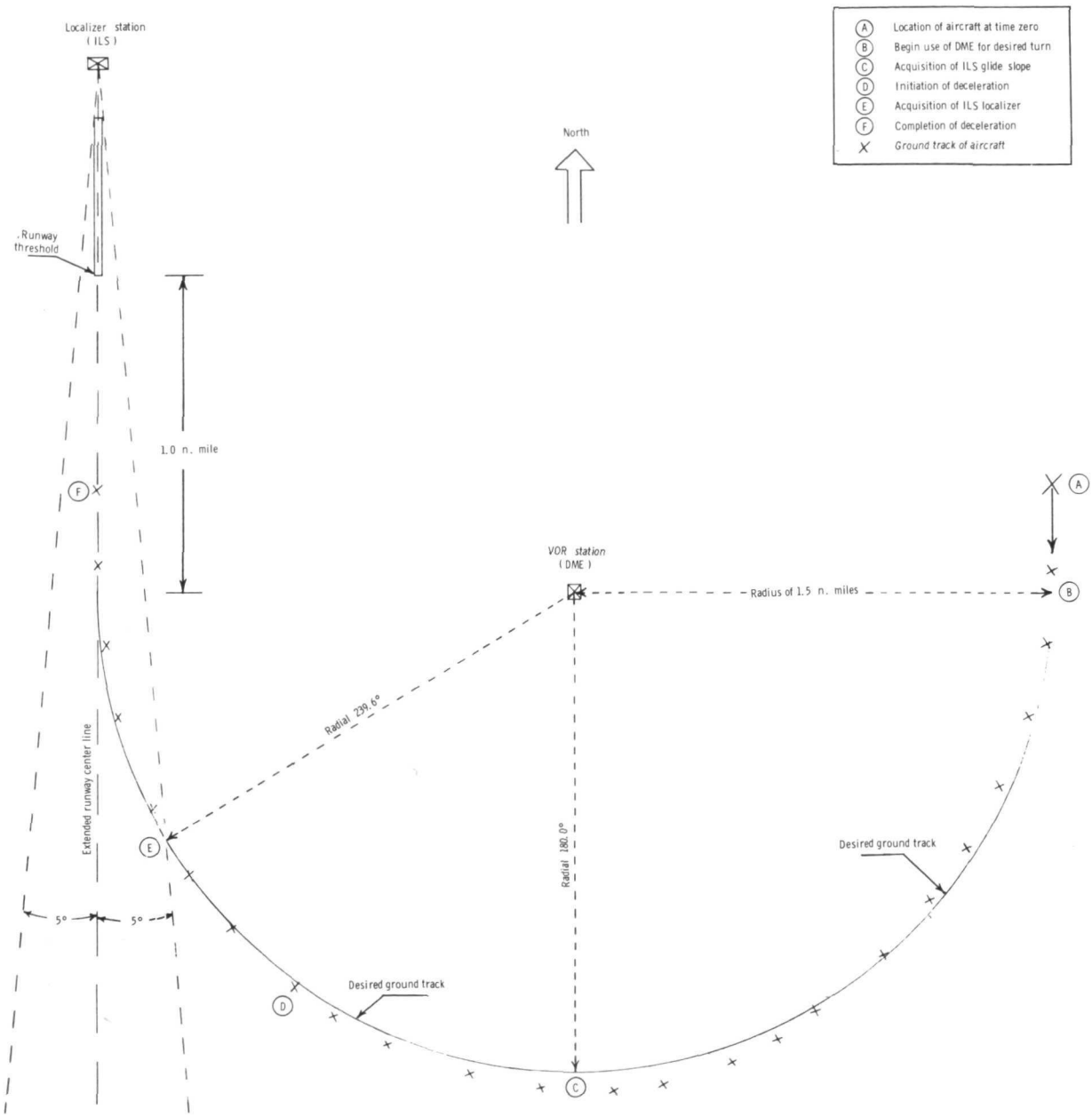

Figure 9.- Ground projection of the simulated curved approach path.

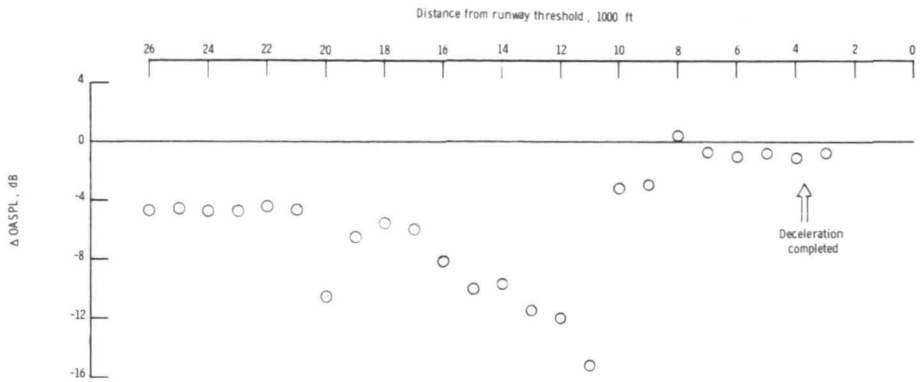

(a) Technique 1.

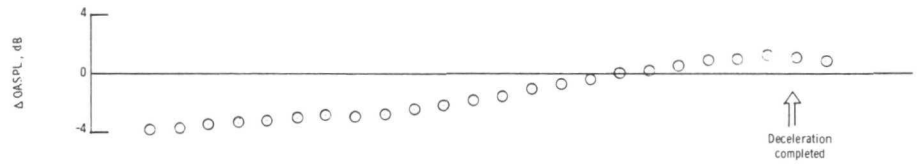

(b) Technique 2.

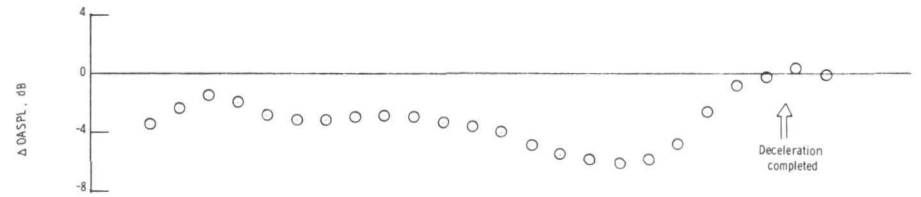

(c) Technique 3.

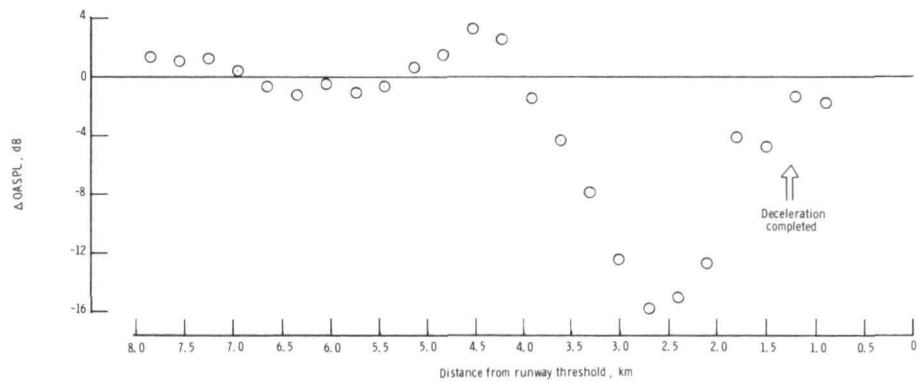

(d) Technique 4.

Figure 10.- Overall sound pressure level for various deceleration techniques as compared with constant airspeed (V = 75 knots) landing approaches. (The deceleration rate used was 0.30 m/sec^2 (1 ft/sec^2).)

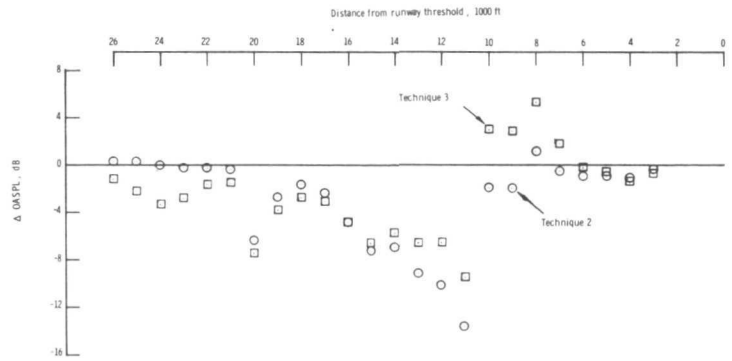

(a) Technique 1 compared with techniques 2 and 3. (Techniques 2 and 3 are used as the references.)

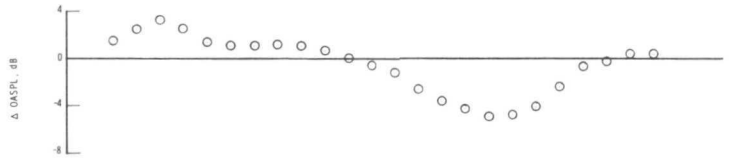

(b) Technique 3 compared with technique 2. (Technique 2 is the reference.)

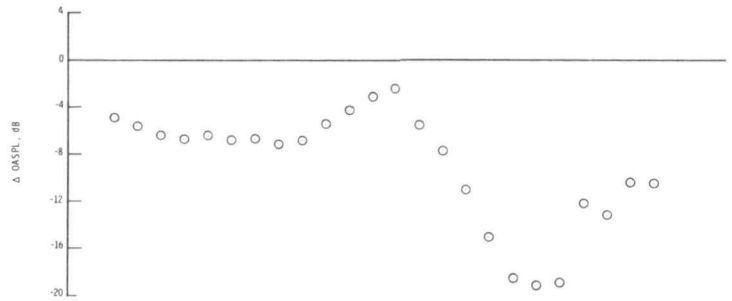

(c) Technique 4 compared with technique 3. (Technique 3 is the reference.)

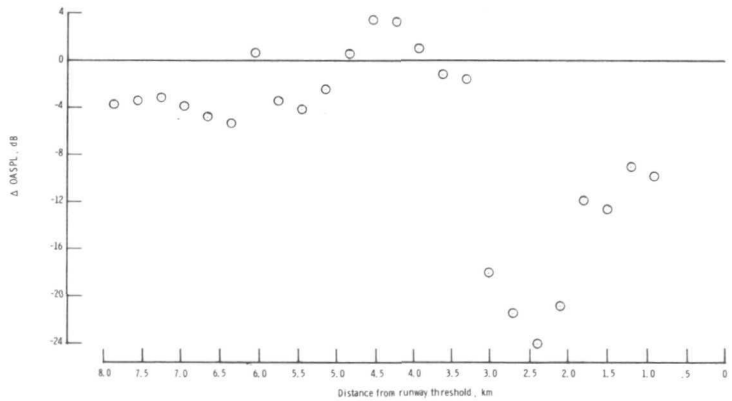

(d) Technique 4 compared with technique 1. (Technique 1 is the reference.)

Figure 11.- Comparison of ground noise levels produced by various deceleration techniques. (The deceleration rate used was 0.30 m/sec^2 (1 ft/sec^2).)

NATIONAL AERONAUTICS AND SPACE ADMINISTRATION
WASHINGTON, D.C. 20546

OFFICIAL BUSINESS
PENALTY FOR PRIVATE USE $300

SPECIAL FOURTH-CLASS RATE
BOOK

POSTAGE AND FEES PAID
NATIONAL AERONAUTICS AND
SPACE ADMINISTRATION
451

U.S.MAIL

POSTMASTER: If Undeliverable (Section 158 Postal Manual) Do Not Return

"The aeronautical and space activities of the United States shall be conducted so as to contribute . . . to the expansion of human knowledge of phenomena in the atmosphere and space. The Administration shall provide for the widest practicable and appropriate dissemination of information concerning its activities and the results thereof."

—NATIONAL AERONAUTICS AND SPACE ACT OF 1958

NASA SCIENTIFIC AND TECHNICAL PUBLICATIONS

TECHNICAL REPORTS: Scientific and technical information considered important, complete, and a lasting contribution to existing knowledge.

TECHNICAL NOTES: Information less broad in scope but nevertheless of importance as a contribution to existing knowledge.

TECHNICAL MEMORANDUMS: Information receiving limited distribution because of preliminary data, security classification, or other reasons. Also includes conference proceedings with either limited or unlimited distribution.

CONTRACTOR REPORTS: Scientific and technical information generated under a NASA contract or grant and considered an important contribution to existing knowledge.

TECHNICAL TRANSLATIONS: Information published in a foreign language considered to merit NASA distribution in English.

SPECIAL PUBLICATIONS: Information derived from or of value to NASA activities. Publications include final reports of major projects, monographs, data compilations, handbooks, sourcebooks, and special bibliographies.

TECHNOLOGY UTILIZATION PUBLICATIONS: Information on technology used by NASA that may be of particular interest in commercial and other non-aerospace applications. Publications include Tech Briefs, Technology Utilization Reports and Technology Surveys.

Details on the availability of these publications may be obtained from:

SCIENTIFIC AND TECHNICAL INFORMATION OFFICE

NATIONAL AERONAUTICS AND SPACE ADMINISTRATION

Washington, D.C. 20546